C1 Turnitin L. R. Telly Savalas

by Lalu Rudyat Telly Savalas C1

Submission date: 21-Feb-2022 12:16PM (UTC+0700)
Submission ID: 1767303268
File name: C01 Disrupted in renal carcinoma 2 (DIRC2) paper October 2011.pdf (1.31M)
Word count: 14302
Character count: 82577

Biochem. J. (2011) **439**, 113–128 (Printed in Great Britain) doi:10.1042/BJ20110166

online data

Disrupted in renal carcinoma 2 (DIRC2), a novel transporter of the lysosomal membrane, is proteolytically processed by cathepsin L

Lalu Rudyat Telly SAVALAS*[1,2], Bruno GASNIER†[1], Markus DAMME‡, Torben LÜBKE§, Christian WROCKLAGE‖, Cécile DEBACKER†, Adrien JÉZÉGOU†¶, Thomas REINHECKEL**, Andrej HASILIK‖, Paul SAFTIG*[3] and Bernd SCHRÖDER*[3]

*Biochemical Institute, Christian-Albrechts-University, Kiel, Germany, †Université Paris Descartes, Centre National de la Recherche Scientifique, UMR 8192 Paris, France, ‡Department of Biochemistry, University of Bielefeld, Bielefeld, Germany, §Biochemistry II, University of Göttingen, Göttingen, Germany, ‖Institute for Physiological Chemistry, Philipps University, Marburg, Germany, ¶Graduate School ED 419, Université Paris-Sud 11, Kremlin-Bicêtre, France, and **Institute for Molecular Medicine and Cell research and Centre for Biological Signalling Studies (bioss), Albert-Ludwigs-University, Freiburg, Germany

DIRC2 (Disrupted in renal carcinoma 2) has been initially identified as a breakpoint-spanning gene in a chromosomal translocation putatively associated with the development of renal cancer. The DIRC2 protein belongs to the MFS (major facilitator superfamily) and has been previously detected by organellar proteomics as a tentative constituent of lysosomal membranes. In the present study, lysosomal residence of overexpressed as well as endogenous DIRC2 was shown by several approaches. DIRC2 is proteolytically processed into a N-glycosylated N-terminal and a non-glycosylated C-terminal fragment respectively. Proteolytic cleavage occurs in lysosomal compartments and critically depends on the activity of cathepsin L which was found to be indispensable for this process in murine embryonic fibroblasts. The cleavage site within DIRC2 was mapped between amino acid residues 214 and 261 using internal epitope tags, and is presumably located within the tentative fifth intralysosomal loop, assuming the typical MFS topology. Lysosomal targeting of DIRC2 was demonstrated to be mediated by a N-terminal dileucine motif. By disrupting this motif, DIRC2 can be redirected to the plasma membrane. Finally, in a whole-cell electrophysiological assay based on heterologous expression of the targeting mutant at the plasma membrane of *Xenopus* oocytes, the application of a complex metabolic mixture evokes an outward current associated with the surface expression of full-length DIRC2. Taken together, these data strongly support the idea that DIRC2 is an electrogenic lysosomal metabolite transporter which is subjected to and presumably modulated by limited proteolytic processing.

Key words: carcinogenesis, cathepsin L, Disrupted in renal carcinoma 2 (DIRC2), lysosomal membrane, major facilitator superfamily, proteolysis.

INTRODUCTION

Lysosomes are membrane-delimited degradative compartments of eukaryotic cells critically important for cellular turnover of exo- and endo-genous macromolecules mainly originating from endocytosis and autophagocytosis respectively [1]. Degradation is performed by more than 50 hydrolases with optimal activity at the acidic luminal pH established by the vacuolar H^+-ATPase residing in the limiting lysosomal membrane.

In contrast with the soluble lysosomal matrix proteins that have been extensively studied and characterized [2], the knowledge on the protein composition of the lysosomal membrane has remained incomplete for much longer. Evidently, a major function of the lysosomal membrane is to form a tight barrier for the lysosomal hydrolases. Concomitantly, such a barrier is also impermeable for the vast majority of low-molecular-mass compounds that are produced by lysosomal breakdown of macromolecules and need to be exported from the lysosome as they would otherwise osmotically destabilize the organelle. For these reasons, the presence of selective transport processes in the lysosomal membrane was postulated long ago. Studies using radiolabelled substrates were able to demonstrate selective saturable translocation of various metabolites, including amino acids, peptides, carbohydrate derivatives, inorganic ions, nucleotides, cobalamine and folylpolyglutamate [3]. Although the specificities and substrate spectrum of some of the transport proteins may partially overlap, it is currently assumed that the lysosomal membrane harbours more than 20 distinct transport proteins, most of them being secondary active driven by the proton gradient [3]. Despite this plethora of functional evidence for lysosomal transporters, only very few have actually been identified and assigned at the protein level.

Several organellar proteomic studies have focussed on the lysosome and identified various novel, previously uncharacterized, proteins along with known lysosomal membrane proteins [2]. Among these candidate proteins with tentative localization in the lysosomal membrane, a number of putative transport proteins have been found. In our previous proteomic study analysing lysosomal membranes from human placenta [4], the putative transport protein DIRC2 (Disrupted in renal carcinoma 2) was confidently identified based on eight unique peptides, and appeared to be enriched in lysosomal membranes according to a spectral-count-based semiquantitative comparative data analysis; however, without meeting the applied criteria of statistical significance.

By homology, DIRC2 belongs to the MFS (major facilitator superfamily), the largest and most diverse family of secondary active transporters [5]. MFS proteins can be found throughout all

Abbreviations used: BYE, bacto yeast extract; DIRC2, Disrupted in renal carcinoma 2; EGFP, enhanced green fluorescent protein; ER, endoplasmic reticulum; FBS, fetal bovine serum; GAPDH, glyceraldehyde-3-phosphate dehydrogenase; GFP, green fluorescent protein; HA, haemagglutinin; HRP, horseradish peroxidase; LAMP, lysosome-associated membrane protein; MEF, murine embryonic fibroblast; MFS, major facilitator superfamily; ORF, open reading frame; PDI, protein disulfide-isomerase; PNGase F, peptide N-glycosidase F; PNS, post-nuclear supernatant; siRNA, small interfering RNA; sulfo-NHS-SS-biotin, sulfosuccinimidyl-2-(biotinamido)ethyl-1,3-dithiopropionate; TLR9, Toll-like receptor 9.

[1] These authors contributed equally to this work.

[2] Present address: Department of Mathematics and Sciences, University of Mataram, Mataram, Indonesia.

[3] Correspondence may be addressed to either of these authors (baschroeder@biochem.uni-kiel.de or psaftig@biochem.uni-kiel.de).

forms of life from bacteria to mankind and it was estimated that approximately 25 % of all known membrane transport proteins in prokaryotes belong to this family [5]. They were shown to transport various low-molecular-mass compounds, metabolites or ions. MFS proteins utilize energy from existing chemi-osmotic gradients [6] and function either as uni-, sym- or anti-porters [5]. The overall sequence homology between individual MFS members is low, and affiliation to this superfamily is mainly based on the presence of certain short sequence signatures, especially in the loop joining transmembrane segments 2 and 3 [5]. Bioinformatic evaluations predict typical MFS proteins to comprise 12 putative transmembrane segments with both their N- and C-termini localized in the cytosol [5]. Structural data, which is only available for a few MFS proteins [7–9], supports this.

The human *DIRC2* gene is located on chromosome 3 and has been identified previously as the breakpoint-spanning gene in a t(2;3)(q35;q21) chromosomal translocation that was found in several affected individuals in a family with hereditary renal cell carcinomas [10]. It was postulated that this translocation, and thereby especially the disruption of the *DIRC2* gene, contributes to the development of renal cancer. However, transcript levels of DIRC2 were normal in all tumour samples tested and, furthermore, no aberrant transcripts or mutations in the remaining allele were detected [10]. Therefore any direct evidence that disruption of one *DIRC2* allele was a causative element during carcinogenesis in these patients is so far missing. Analysis of the *DIRC2* expression pattern at the mRNA level has revealed ubiquitous expression with slightly higher levels in placenta and heart [10].

In the present study, we have corroborated the hypothesis raised by proteomics analysis [4] that DIRC2 is a novel lysosomal transport protein and performed an in-depth biochemical and cell biological analysis. We confirm the lysosomal residence of overexpressed as well as endogenous DIRC2 and demonstrate that DIRC2 carries N-glycans at Asn^{209}, and that its lysosomal targeting critically depends on a N-terminally located dileucine motif. Furthermore, the results show that DIRC2 is proteolytically processed subsequent to its delivery to lysosomal compartments. For this processing, cathepsin L is of critical importance. Functional studies in *Xenopus* oocytes based on a dileucine-targeting mutant indicate that DIRC2 is an electrogenic metabolite transporter, in agreement with its homology with MFS proteins.

EXPERIMENTAL

Reagents and antibodies

Brefeldin A, leupeptin and pepstatin A were purchased from Sigma–Aldrich; E-64 and CA-074 Me were from Enzo Life Sciences; and Z-FY-CHO was from Calbiochem/Merck.

Monoclonal antibodies against GFP (green fluorescent protein) and the HA (haemagglutinin) epitope tag (3F10) were purchased from Roche. A mouse monoclonal antibody (9B11) and a rabbit polyclonal antibody against the Myc epitope tag were from Cell Signaling Technology and Santa Cruz Biotechnology respectively. A polyclonal rabbit antiserum against cathepsin D has been described previously [11], as has a monoclonal antibody against h-LAMP2 (human lysosome-associated membrane protein 2) [12]. A monoclonal antibody directed against the ER (endoplasmic reticulum)-retention motif 'KDEL' was obtained from Stressgen. Anti-PDI (protein disulfide-isomerase) antibody was purchased from Santa Cruz Biotechnology. Anti-β-tubulin (E7) and anti-m-LAMP2 (mouse LAMP2) (ABL-93) were from Developmental Studies Hybridoma Bank. A polyclonal antibody against murine cathepsin L was obtained from R&D Systems. Polyclonal antibodies against actin and GAPDH (glyceraldehyde-3-phosphate dehydrogenase) were from Sigma–Aldrich. Fluorochrome-conjugated secondary antibodies (anti-rat IgG and anti-rabbit IgG coupled to Alexa Fluor® 488, and anti-mouse IgG and anti-rat IgG coupled to Alexa Fluor® 594) were purchased from Molecular Probes (Invitrogen). For immunoblotting, secondary antibodies coupled to HRP (horseradish peroxidase) were used (Dianova).

A specific antiserum was raised against a synthetic peptide comprising residues 2–19 of human DIRC2 protein (GSRWSSEEERQPLLGPGL). Peptide synthesis, coupling to keyhole limpet haemocyanin, immunization of rabbits and affinity purification of antiserum against the immobilized peptide were performed by Pineda Antikörper-Services according to standard procedures.

Cloning of expression constructs

Human *DIRC2* cDNA (clone: IRATp970A0572D) was obtained from ImaGenes. A schematic illustration of the expression constructs used is shown in Figure 1(C). Constructs with N- and C-terminally appended GFP were generated in peGFP-C1 and peGFP-N1 (Clontech) vectors respectively. The DIRC2 ORF (open reading frame) was amplified using either DIRC2-GFP-N1-Fw (5′-CAGAGCTCAGCCACCATGGGCTCTCGCTGGAGCA-3′) and DIRC2-GFP-N1-Rv (5′-TCGGATCCTGGTCGACAACGGAGACAACCACATCAAGAT-3′) or DIRC2-GFP-C1-Fw (5′-CAGTCAAGATCTATGGGCTCTCGCTGGAGCA-3′) and DIRC2-GFP-C1-Rv (5′-TAGAATTCTTAAACGGAGACAACCACAT-3′) respectively. PCR products were subcloned into peGFP-N1 and peGFP-C1 after restriction digestion with SacI/BamHI and BglII/EcoRI respectively.

An expression construct with a triple Myc tag fused to the C-terminus of DIRC2 (DIRC2–3×Myc-pcDNA3.1/Hygro+) was generated by amplification of the ORF with DIRC2-pcDNA3.1-Fw (5′-GTACTAAAGCTTGCCACCATGGGCTCTCGCTGGAGCA-3′) and DIRC2-3xMyc-Rv (5′-GATCCTCGAGTTACAGATCCTCTTCTGAGATGAGTTTTTGTTCCAGATCCTCTTCTGAGATGAGTTTTTGTTCCAGATCTTCTTCAGAAATAAGTTTTTGTTCGGATCCAACG-3′) and subcloning of the PCR product into pcDNA3.1/Hygro+ (Invitrogen) using HindIII and XhoI sites.

A mutation of the N-glycosylation site Asn^{209} (N209A) was introduced into the DIRC2 ORF by overlap-extension PCR using N209A-Fw (5′-GCTCCCGCAGGGACGTCACCTCTTCTTGCTGCA-3′) and N209A-Rv (5′-TGACGTCCCTGCGGGAGCTGGAACAACAAGTGGTCC-3′) as internal primers as well as DIRC2-pcDNA3.1-Fw and DIRC2-3xMyc-Rv as flanking primers. For the lysosomal-targeting mutant LL14/15AA LL/AA-Fw (5′-GCGAAGAGGAGAGGCAGCCAGCTGCGGGGCCCGGGCTCGGGCCTG-3′) and LL/AA-Rv (5′-CAGGCCCGAGCCCGGGCCCCGCAGCTGGCTGCCTCTCCTCTTCGC-3′) were used as internal primers. In order to generate an ER-retention mutant of DIRC2, the 14 C-terminal amino acid residues of the human α2C adrenergic receptor (KHILFRRRRRGFRQ) [13] were fused to the C-terminus of the triple Myc tag in DIRC2–3×Myc which was achieved by amplification with DIRC2-pcDNA3.1-Fw and DIRC2-ER-Rv (5′-GATCTCTAGATCACTGCCTGAAGCCTCTTCTCCTCCGTCGAAAATAGTATGTGCTTTCTCGAGTTCAGATCCTCTTC-3′) from the template DIRC2–3×Myc and subcloning via HindIII/XbaI sites into pcDNA3.1/Hygro+.

In order to allow mapping of the proteolysis site, internal HA tags were introduced into DIRC2–3×Myc-pcDNA3.1/Hygro+ after amino acids 214 and 261 of the DIRC2 ORF respectively,

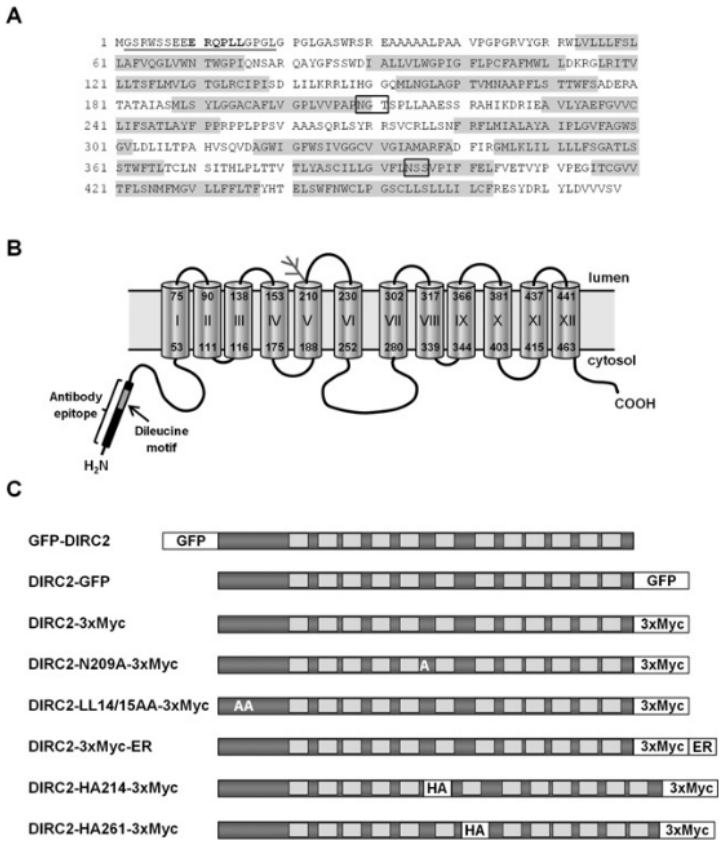

Figure 1 Bioinformatic analysis of DIRC2

(**A**) Amino acid sequence of human DIRC2 protein. Stretches of amino acids representing predicted transmembrane segments are shaded in grey and the epitope used for antibody generation is underlined. Positions of the dileucine motif critically involved in lysosomal targeting of DIRC2 (LL14/15) and putative consensus sites for N-glycosylation are marked by bold letters and boxes respectively. (**B**) Topology of DIRC2 with 12 putative transmembrane segments and cytosolic localization of N- and C-termini according to prediction by TMHMM (http://www.expasy.org). The transmembrane segments are numbered in roman. Positions of the epitope used for antibody generation, the critical dileucine motif LL14/15 and the experimentally confirmed N-glycosylation site Asn^{209} (the branched symbol) are indicated. (**C**) Schematic diagram of DIRC2 constructs used for expression in mammalian cells. Positions of the in-frame fused GFP, HA and Myc tags used for the detection of the protein and its fragments are indicated.

by overlap-extension PCR. As internal primers HA214-FW (5′-CATACGACGTCCCAGACTACGCTCTTGCTGCAGAGAGC-AGCAG-3′) and HA214-Rv (5′-TAGTCTGGGACGTCGTATG-GGTAAAGAGGTGATGTCCCATTG-3′) or HA261-FW (5′-C-ATACGACGTCCCAGACTACGCGGCAGCTAGCCAGCGG-CTGAG-3′) and HA261-RV (5′-TAGTCTGGGACGTCGTAT-GGGTAAGCAACACTGGGAGGAAGAG-3′) were used in combination with DIRC2-pcDNA3.1-Fw and DIRC2–3×Myc-Rv as flanking primers. PCR products were subcloned via HindIII and XhoI sites into pcDNA3.1/Hygro+.

For expression in *Xenopus* oocytes, inserts encoding wild-type DIRC2–EGFP (enhanced GFP) or the corresponding LL14/15AA mutant were excised from the aforementioned peGFP-N1 constructs using BamHI and NotI enzymes, and subcloned at the BglII and NotI sites of the pOX(+) vector [14], a kind gift of Dr M. Hediger (University of Bern, Bern, Switzerland). This vector allows high expression levels in frog oocytes owing to the presence of 5′ and 3′ non-coding sequences from *Xenopus laevis* β-globulin mRNA flanking the polylinker region. After linearization of the pOX(+) constructs at the SwaI site, capped cRNAs were synthesized *in vitro* using the mMessage-mMachine SP6 kit (Ambion).

Cell culture and transfection

HeLa cells were purchased from DSMZ. MEFs (murine embryonic fibroblasts) derived from cathepsin $L^{-/-}$ [15], cathepsin $B^{-/-}$ [16], cathepsin $B^{-/-}$/cathepsin $L^{-/-}$ [17] and cathepsin $D^{-/-}$ [18] mice have been described previously. Cells were maintained in DMEM (Dulbecco's modified Eagle's medium; PAA) supplemented with 10% (v/v) FBS (fetal bovine serum; PAA), 100 units/ml penicillin (PAA) and 100 mg/ml streptomycin (PAA) in a humidified 5% CO_2/air atmosphere at 37 °C.

In order to achieve 30–50% confluency of HeLa cells and 60–80% of MEFs at the time of transfection, cells were seeded 24 h in advance. Expression plasmids were transfected using Turbofect (Fermentas) according to the manufacturer's instructions, with 2.5 μg and 0.5 μg of DNA for a 10 cm and 3.5 cm dish of HeLa cells, and 10 μg of DNA for a 10 cm dish of MEFs.

Transient down-regulation of DIRC2 in HeLa cells was performed with Stealth Select RNAi™ (Invitrogen) siRNA (small interfering RNA): HSS131473 (5′-GGAGGCUGUGUUGUU-GGAAUAGCUA-3′), HSS131474 (5′-UCUUGAAUAGCAG-CGUGCCUAUAUU-3′), HSS131475 (5′-GCAGAAUUUGGA-GUUGUCUGCUUAA-3′). DIRC2 siRNA as well as suitable

non-targeting control siRNAs were transfected with INTERFERin™ (Polyplus transfection) according to the manufacturer's recommendations, with a final concentration of 10 nM siRNA in the culture medium.

Indirect immunofluorescence

Cells adherent to coverslips were fixed with 4 % (w/v) paraformaldehyde in PBS for 20 min. After permeabilization with 0.2 % saponin in PBS, non-specific binding of antibodies was prevented by pre-incubating the coverslips in 10 % FCS in PBS supplemented with 0.2 % saponin (FBS/PBS/Sap). Primary and secondary antibodies were diluted in FBS/PBS/Sap and applied overnight at 4 °C and for 1 h at room temperature (22 °C) in a humidified chamber. Nuclei were stained with DAPI (4′,6-diamidino-2-phenylindole, Sigma–Aldrich) which was included in the embedding medium. Specimens were documented with an Axiovert 200M fluorescence microscope (Zeiss) equipped with an Apotome for optical sectioning.

Protein extraction and immunoblotting

Cultured cells were harvested by scraping into PBS and cells were sedimented at 1000 ***g*** for 5 min. Pelleted cells were extracted in lysis buffer [50 mM Tris/HCl (pH 7.4), 150 mM NaCl, 1.0 % (w/v) Triton X-100, 0.1 % SDS and 4 mM EDTA] supplemented with protease inhibitors as described in [19]. Samples were sonicated (level 4 for 20 s using a Branson Sonifier 450 at 4 °C) and incubated on ice for 1 h. Lysates were cleared by centrifugation (15000 ***g***, 10 min) and the protein concentration was determined with a BCA (bicinchoninic acid) protein assay kit (Thermo Scientific). Pools of five *Xenopus* oocytes were solubilized 2 days after cRNA injection (see below) in 300 mM NaCl, 1.5 mM $MgCl_2$, 1 mM EDTA and 20 mM Hepes-NaOH (pH 7.5) supplemented with 20 % (v/v) glycerol, 10 mM DTT (dithiothreitol) and 0.2 % Nonidet P40. After repeated pipetting for 2 min at room temperature, lysates were chilled and centrifuged for 5 min at 16000 ***g***. Supernatants were frozen in liquid nitrogen before immunoblot analysis. SDS/PAGE [20], semi-dry transfer on to nitrocellulose and immunodetection were carried out as described previously [19]. In order to prevent aggregation of the highly hydrophobic DIRC2 protein, the boiling step was omitted and samples were incubated for 15 min at 37 °C instead.

Deglycosylation by PNGase F (peptide N-glycosidase F)

Deglycosylation by PNGase F was performed as described previously [19], with the only difference being that samples were denatured by incubation at 56 °C for 5 min instead of 95 °C. Controls were treated equivalently, except that the glycosidase was omitted.

Surface biotinylation and streptavidin pull down

In transfected HeLa cells, cell-surface proteins were labelled with the membrane impermeable, cleavable reagent sulfo-NHS-SS-biotin [sulfosuccinimidyl-2-(biotinamido)ethyl-1,3-dithiopropionate; Thermo Scientific] 48 h after transfection. The monolayer was washed three times with ice-cold PBS and then incubated in the presence of 1 mg/ml sulfo-NHS-SS-biotin dissolved in PBS for 60 min at 4 °C. Residual biotin was removed by washing with PBS and a 10 min incubation in 50 mM Tris/HCl (pH 7.4), in PBS at 4 °C. Aliquots of total cell lysates (450 μg of protein) were subjected to pull down with 50 μl of high-capacity streptavidin-agarose resin (Thermo Scientific) for 1 h at 4 °C. After five washing steps (1 ml each of lysis buffer), bound biotinylated proteins were eluted in 100 μl of reducing SDS/PAGE sample buffer by incubation for 5 min at 56 °C followed by 30 min at 37 °C. For Western blot analysis, aliquots of the total lysates ('T', 15 μg of protein), the streptavidin pull-down supernatant containing unbound protein ('U', corresponding to 15 μg of protein prior to pull down) and 50 μl of the eluted biotinylated proteins ('B') were subjected to SDS/PAGE.

Similarly, five *Xenopus* oocytes were surface-biotinylated 2 days after injection using 2.5 mg/ml sulfo-NHS-SS-biotin in PBS for 20 min at 4 °C. After six washes, oocytes were lysed for 30 min in 500 μl of lysis buffer [150 mM NaCl, 5 mM EDTA, 50 mM Tris/HCl (pH 7.5), 0.1 % SDS, 1 % Triton X-100, 1 mM PMSF, 0.1 mM leupeptin and 0.1 μM pepstatin A]. Lysates were subjected to pull down with 150 μl of streptavidin-agarose beads (Fluka) for 2 h at 4 °C, and beads were washed three times with 1 ml of lysis buffer. Finally, streptavidin-bound protein was eluted in 100 μl of SDS/PAGE sample buffer. Half of the bound proteins and 5 % of the cell lysate or unbound material were resolved by SDS/PAGE and analysed by immunoblotting using an anti-GFP antibody.

Metabolic labelling and immunoprecipitation

HeLa cells grown in six-well plates were transfected as described above and incubated for 7 h under standard conditions followed by 30 min in serum-free medium. Subsequently, the cells were metabolically labelled with 9 MBq of [^{35}S]methionine/cysteine mixture (Hartmann Analytic) diluted in cysteine-, methionine-free RPMI 1640 medium supplemented with 5 % (v/v) FBS dialysed against 0.9 % NaCl. Cells from one well were harvested directly after a 2.5 h incubation (pulse). The remaining wells were incubated in fresh culturing medium for chase periods of 3, 11 and 19 h. Cells were recovered as described above and pellets were homogenized in 0.75 ml of 10 mM Tris/HCl (pH 7.4) containing 0.1 % SDS and protease inhibitors at room temperature. Triton X-100, $MgCl_2$ and bovine pancreatic DNase were added to final concentrations of 1 % (v/v), 1 mM and 0.1 mg/ml respectively. After 10 min, EDTA, *p*-aminobenzamidine and *Staphylococcus aureus* cell walls (Pansorbin®, Calbiochem) were added to achieve 2 mM, 1 mM and 0.5 % concentrations respectively. The samples were mixed by rotation for 45 min at 4 °C and subjected to centrifugation at 40000 ***g*** for 20 min. Supernatants were then immunoprecipitated with an anti-Myc antibody (9B11) in combination with rabbit anti-mouse IgG antiserum. Immune complexes were recovered by pull down with 0.5 % *S. aureus* cell walls, washed as described previously [21] and eluted in reducing SDS/PAGE sample buffer. Labelled protein was visualized by fluorography after separation by SDS/PAGE.

Lysosome isolation from mouse liver (tritosomes)

Animal experimentation was performed in agreement with local and national guidelines for use of animals and their care. Lysosomes from mouse liver were isolated using an established density-shift procedure involving intravenous application of the non-ionic detergent tyloxapol (Triton WR1339; Sigma–Aldrich) resulting in VLDL (very-low-density lipoprotein)- and tyloxapol-filled lysosomes ('tritosomes') that exhibit a markedly reduced buoyant density. Wild-type and cathepsin-L-deficient mice were injected with 0.75 mg of tyloxapol/g of body weight 4 days prior to being killed and removal of the livers. A tritosome-enriched fraction ('ML') was obtained from liver homogenates by differential centrifugation and further purified by isopycnic centrifugation in a sucrose step gradient which was divided into

four fractions (F1–F4) after centrifugation, with F2 being the fraction with the highest lysosomal/tritosomal enrichment [22].

Lysosomal membrane isolation from human placenta

Lysosomes were isolated from human placenta as described previously [12]. A placental homogenate was fractionated by differential centrifugation followed by centrifugation in a self-forming Percoll® density gradient. A lysosome-enriched subfraction ('dense pool') was recovered from the bottom third of the gradient. In order to deplete Percoll® and soluble lysosomal proteins, the 'dense pool' was diluted in 10 mM Tris/HCl (pH 7.4), sonicated (level 4 for 20 s using a Branson Sonifier 450 at 4 °C) and membranes were recovered by ultracentrifugation for 2 h at 50000 rev./min (rotor type 60 Ti; Beckman) followed by one step of washing in the same buffer under the same conditions of centrifugation.

Subcellular fractionation of cultured cells

HeLa cells and MEFs were grown in 10 cm dishes. The cell monolayer was washed twice with PBS, twice with homogenization buffer [250 mM sucrose, 10 mM Hepes-NaOH (pH 7.4) and 1 mM EDTA] and scraped into 1 ml of homogenization buffer, from which cells were recovered by centrifugation (250 ***g***, 5 min). HeLa cells were resuspended in 1 ml of fresh homogenization medium and mechanically disrupted with 16 passages through a 27-gauge cannula fitted to a 1 ml syringe. MEFs were resuspended and briefly incubated in 500 μl of 10 mM Hepes-NaOH (pH 7.4) under hypotonic conditions and disrupted by ten passages through a 27-gauge cannula. Immediately, 500 μl of 500 mM sucrose, 10 mM Hepes-NaOH (pH 7.4) and 2 mM EDTA was added and cells were passed through the cannula six more times. Homogenates were centrifuged for 10 min at 1000 ***g*** to obtain the PNS (post-nuclear supernatant).

PNS from HeLa cells was further separated by density-gradient centrifugation using a self-forming Percoll® density gradient as described previously [19]. After centrifugation, fourteen fractions were collected from the top to the bottom of the gradient. In all fractions activities of β-hexosaminidase [23] and alkaline phosphatase [24] were determined with spectrophotometric assays. Aliquots of equal volume from each fraction were analysed by Western blotting.

Total cellular membranes from MEFs were obtained by centrifugation of the PNS at 50000 rev./min (rotor type TLA-55; Beckman) for 1 h at 4 °C. In order to further enrich integral membrane proteins, membranes were resuspended in 100 mM Na_2CO_3 (pH 11.5), incubated for 1 h on ice and recovered by centrifugation at 50000 rev./min (rotor type TLA-55; Beckman) for 1 h at 4 °C. After one step of washing in 10 mM Hepes-NaOH (pH 7.4), the membrane pellet was resuspended in this buffer and used for Western blot analysis.

Electrophysiological measurements in *Xenopus* oocytes

Ovarian lobes were extracted from *X. laevis* females under anaesthesia and oocyte clusters were incubated on a shaker in OR2 medium [85 mM NaCl, 1 mM $MgCl_2$ and 5 mM Hepes-KOH (pH 7.6)] containing 2 mg/ml collagenase type II (Gibco) for 1 h at room temperature. Defolliculated oocytes were sorted and kept at 19 °C in Barth's solution [88 mM NaCl, 1 mM KCl, 2.4 mM $NaHCO_3$, 0.82 mM $MgSO_4$, 0.33 mM $Ca(NO_3)_2$, 0.41 mM $CaCl_2$ and 10 mM Hepes-NaOH (pH 7.4)], supplemented with 50 μg/ml gentamicin. Oocytes were injected with 50 ng of cRNA using a nanolitre injector (World Precision Instruments). Expression of EGFP-tagged constructs at the oocyte surface was verified under an Eclipse TE-2000 epifluorescence microscope (Nikon) with a 4× objective lens and was used to preselect oocytes with the highest expression levels for electrophysiological recording. Epifluorescence micrographs, focused on the equatorial plane of oocytes, were acquired under identical exposure conditions with a CCD (charge-coupled-device) camera (Coolsnap) and processed using ImageJ.

At 2 days after cRNA injection, currents were recorded at room temperature under voltage clamp using an O-725A amplifier (Warner Instrument), a Digidata 1200 interface and the pClamp software (Molecular Devices), two intracellular borosilicate-glass microelectrodes filled with 3M KCl (0.3–2 MΩ tip resistance) and an Ag/AgCl reference electrode located close to the oocyte. Impaled oocytes were perfused with ND100 solution [100 mM NaCl, 2 mM KCl, 1 mM $MgCl_2$, 1.8 mM $CaCl_2$ and 5 mM Hepes or Mes (adjusted to pH 7.0 or 5.0 respectively with CsOH)]. After equilibration of the oocyte conductance at pH 5.0, ND100 solution supplemented with 5 % (w/v) BYE (bacto yeast extract; Becton Dickinson) and adjusted to the same pH was applied for ~50 s, and subsequently washed away. Current traces, acquired at a constant holding potential (− 40 mV), were filtered at 200 Hz and sampled at 500 Hz. Data were analysed offline using Clampfit 9 (Molecular Devices).

RESULTS

Bioinformatic analysis of DIRC2

The human DIRC2 protein comprises 478 amino acids (Figure 1A) corresponding to a calculated molecular mass of 52.1 kDa. Sequence analysis *in silico* (TMHMM, http://www.expasy.org) revealed twelve putative transmembrane segments (Figure 1A) and a topology with cytosolic localization of the N- and C-termini (Figure 1B) without a cleavable N-terminal signal sequence (SignalP, http://www.expasy.org). Two consensus sites for N-glycosylation are present within the DIRC2 sequence: Asn^{209} and Asn^{394} (Figure 1A, boxes) with the latter being unlikely to be in use since it is localized within a predicted transmembrane segment. Candidates for lysosomal-targeting motifs are found at the N- and C-termini of DIRC2 respectively. Whereas the N-terminus contains a potential dileucine motif $E^{10}RQPLL^{15}$, the C-terminus harbours two putative tyrosine-based sorting motifs: $Y^{467}DRL^{470}$ and $Y^{471}LDV^{474}$. Between predicted transmembrane segment 2 and 3, DIRC2 features a sequence stretch characteristic for the MFS, suggesting DIRC2 to be a member of this superfamily. Furthermore, the predicted topology of DIRC2 with 12 densely packed transmembrane segments is in agreement with the typical structure of MFS proteins [7].

DIRC2 is a lysosomal membrane protein

Lysosomal localization of DIRC2 had been suggested by an organellar proteomic study [4]. For validation, fusion proteins of DIRC2 with GFP at either end of the protein (Figure 1C) were transiently overexpressed in HeLa cells. Both fusion proteins (GFP–DIRC2 and DIRC2–GFP) were observed in intracellular vesicles co-localizing with LAMP2, a marker of lysosomal/late endosomal compartments (Figure 2A). Since GFP can induce mistargeting of proteins, a construct with a C-terminally appended triple Myc tag (DIRC2–3×Myc) was generated, and the subcellular distribution of the respective fusion protein was examined. Co-localization with LAMP2 (Figure 2A), as well as cathepsin D, β-glucocerebrosidase, the late endosomal

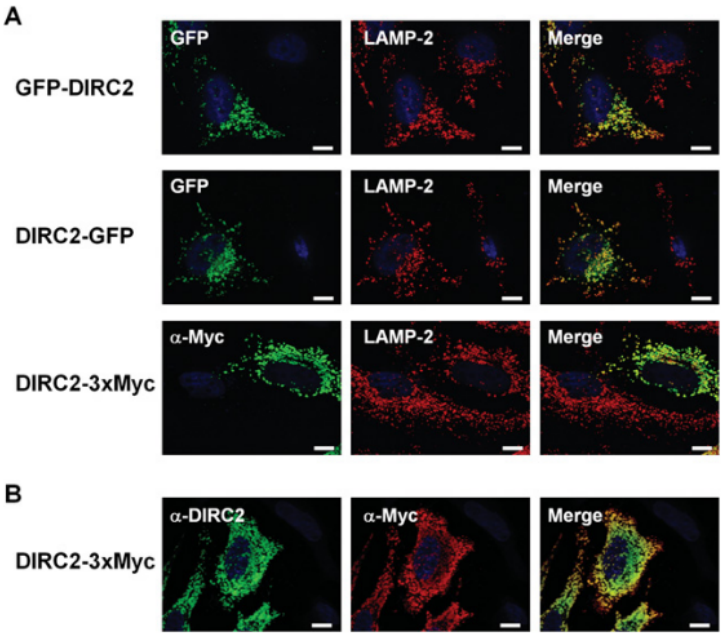

Figure 2 Overexpressed DIRC2 localizes to lysosomes in HeLa cells

HeLa cells transiently expressing DIRC2-peGFP-C1 (GFP–DIRC2), DIRC2-peGFP-N1 (DIRC2–GFP) or DIRC2–3×Myc-pcDNA3.1/Hygro + (DIRC2–3×Myc) were fixed 24 h after transfection. The distribution of DIRC2-fusion proteins was monitored based on GFP fluorescence (**A**) or by indirect immunofluorescence using an anti-Myc antibody (**B**). In parallel, lysosomes were visualized by co-staining of the lysosomal marker protein LAMP2. Lysosomal localization was observed for all DIRC2-fusion proteins analysed independently of the nature of the epitope tag and its localization at the N-or the C-termini. (**B**) HeLa cells transiently expressing DIRC2 with a C-terminally appended triple Myc tag (DIRC2–3×Myc) were fixed 48 h after transfection and localization of DIRC2 was assessed by indirect immunofluorescence. Co-staining was performed with the monoclonal anti-Myc antibody (9B11) and polyclonal anti-DIRC2 antibody raised against a synthetic peptide from the N-terminal part of DIRC2. Co-localization of both signals was observed, thus validating the specificity of the anti-DIRC2 antibody. Scale bars represent 10 μM.

lipid bis(monoacylglycero)phosphate and acidic compartments visualized by staining with lysotracker (results not shown), was observed. In order to allow detection of endogenous DIRC2 protein, an antiserum was generated against a synthetic peptide corresponding to the N-terminus of DIRC2 (Figures 1A and 1B). In HeLa cells transiently expressing DIRC2–3×Myc, the staining pattern obtained with this antibody was similar to that achieved with the anti-Myc antibody, demonstrating the specificity of the antibody generated (Figure 2B). No specific staining was observed in non-transfected HeLa cells, indicating that the endogenous expression level is too low to be detected with this antibody in immunocytochemistry, in contrast with Western blotting (Figure 4A).

DIRC2 is proteolytically processed and N-glycosylated at Asn^{209}

Surprisingly, Western blot analysis of cells expressing the GFP-fusion constructs shown in Figure 2(A) revealed divergent band patterns depending on whether GFP was fused to the N- or to the C-terminus of DIRC2 (Figure 3A). Based on the theoretical molecular mass of DIRC2 of 52 kDa and 27 kDa for GFP, such a fusion protein would be expected at approximately 80 kDa. However, the major bands were observed between 40 and 50 kDa for GFP–DIRC2 and at approximately 40 kDa for DIRC2–GFP, and are therefore unlikely to represent full-length DIRC2 fused to GFP. Discrepancies between the apparent molecular mass in SDS/PAGE and the actual size of a protein are conceivable, but are unable to account for the incongruent patterns obtained for GFP–DIRC2 and DIRC2–GFP. Instead, these findings were highly suggestive of a proteolytic processing event resulting in N- and C-terminal fragments of DIRC2.

In order to avoid possible artefacts associated with GFP, further analyses were performed with the DIRC2–3×Myc expression construct introduced above. Total lysates from HeLa cells transiently expressing DIRC2–3×Myc were analysed by Western blotting using anti-DIRC2 (N-terminal epitope) and anti-Myc (C-terminus) antibodies for the detection of full-length DIRC2 as well as putative fragments. Furthermore, possible N-glycans were removed by treatment with PNGase F (Figure 3B). In agreement with the previous findings, the bulk of overexpressed DIRC2–3×Myc was present in proteolytically processed form, detectable as N- and C-terminal fragments (open arrowhead). After deglycosylation, a band slightly below 55 kDa was observed upon detection with either antibody, presumably representing full-length DIRC2 (closed arrowhead). Removal of N-glycans resulted in a reduction of the apparent molecular mass of both full-length DIRC2 and its N-terminal fragment (open arrowhead), whereas the electrophoretic mobility of the C-terminal fragment was not changed (Figure 3B, 'anti-Myc', open arrowhead). The band representing the N-terminal fragment of DIRC2 (Figure 3B, upper panel, lane 3, open arrowhead) appears to be very broad, indicating a pronounced heterogeneity in terms of molecular mass. Since only one discrete band is observed for the N-terminal fragment after deglycosylation (lane 4), this heterogeneity can be attributed to different branching of the attached oligosaccharides rather than to different sites of proteolysis.

As discussed above, out of two 'NXS/T' consensus sites, only Asn^{209} is likely to be utilized for N-glycosylation. A mutant construct DIRC2-N209A was analysed and found to be

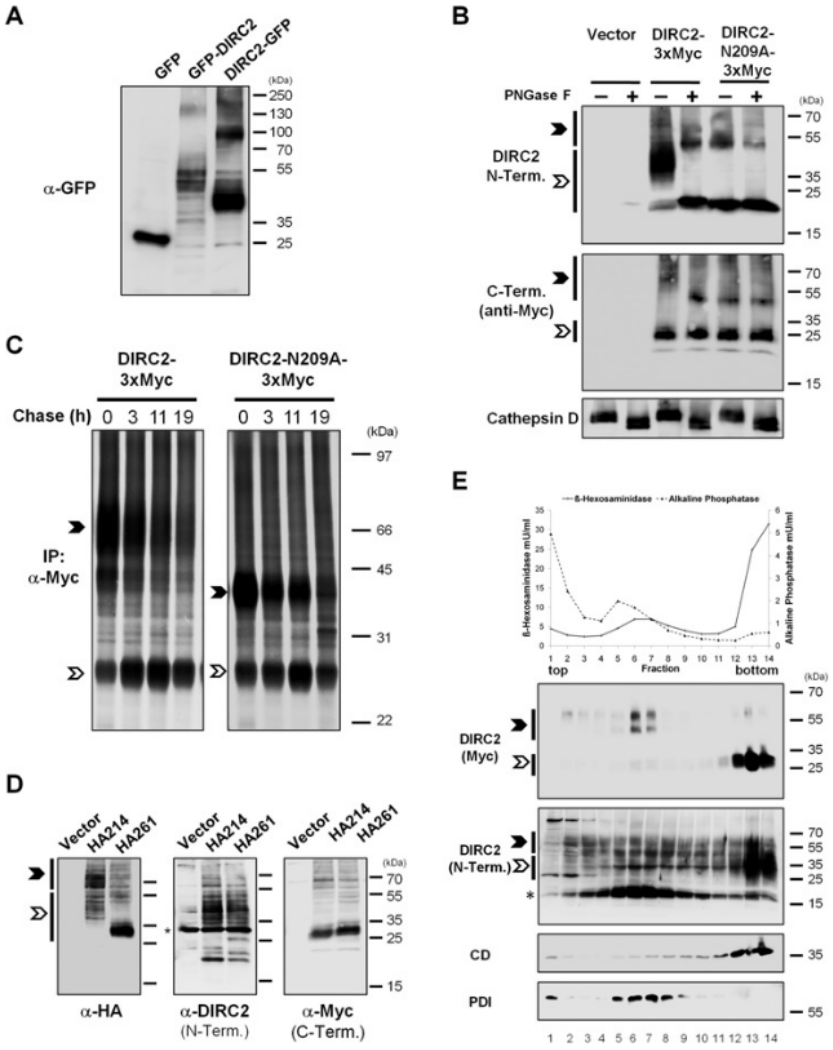

Figure 3 Post-translational modification and processing of DIRC2

(**A**) HeLa cells were transiently transfected with DIRC2-peGFP-C1 (GFP–DIRC2), DIRC2-peGFP-N1 (DIRC2–GFP) or empty peGFP-N1 (GFP). Cells were harvested 48 h after transfection. Total cell lysates (20 μg of protein) were subjected to SDS/PAGE and Western blot analysis. Membranes were probed with an anti-GFP antibody followed by a HRP-conjugated secondary antibody. (**B**) HeLa cells were transiently transfected with DIRC2–3×Myc-pcDNA3.1/Hygro+ (DIRC2–3×Myc), mutant DIRC2-N209A–3×Myc-pcDNA3.1/Hygro+ (DIRC2-N209A) or empty pcDNA3.1/Hygro+. Total cell lysates were prepared 48 h after transfection and aliquots (20 μg of protein) were incubated in the absence (−) or presence (+) of PNGase F. Samples were analysed by SDS/PAGE and Western blotting using an anti-DIRC2 antibody directed against an N-terminal epitope of DIRC2, anti-Myc antibody binding to the C-terminally appended triple Myc tag and anti-cathepsin D antibody as a positive control. Positions of full-length DIRC2 and the proteolytic fragments (N- or C-terminal respectively) are indicated by closed and open arrowheads respectively. (**C**) HeLa cells were transiently transfected with DIRC2–3×Myc-pcDNA3.1/Hygro+ (DIRC2–3×Myc) or DIRC2-N209A–3×Myc-pcDNA3.1/Hygro+ (DIRC2-N209A–3×Myc). At 8 h after transfection, cells were metabolically pulse-labelled with a [^{35}S]methionine/cysteine mixture for 2.5 h. Subsequently, the labelling was chased by incubating the cells in fresh culturing medium with radioactive label for the indicated times prior to harvest. Total lysates were prepared and subjected to immunoprecipitation using an anti-Myc antibody. The recovered immune complexes were separated by SDS/PAGE and visualized by fluorography. The positions of full-length DIRC2 and the C-terminal fragment are marked with closed and open arrowheads respectively. (**D**) DIRC2 expression constructs with internal HA tags at amino acid positions 214 and 261 respectively, and triple Myc tag at the C-terminus were transiently expressed in HeLa cells. Cells were harvested 48 h after transfection and total lysates were analysed by Western blotting (40 μg of protein per lane). Membranes were probed with anti-DIRC2, anti-Myc or anti-HA antibodies in order to detect the N- or C-terminus of DIRC2 or the inserted internal HA tag respectively. Closed and open arrowheads mark positions of bands representing full-length and proteolytically processed (N- or C-terminal fragments respectively) DIRC2. An asterisk indicates an non-specific band unrelated to DIRC2 expression. The differential band patterns observed with the anti-HA antibody for both DIRC2 constructs suggest that proteolytic processing of DIRC2 occurs between amino acids 214 and 261. (**E**) Subcellular fractionation of HeLa cells transiently expressing DIRC2–3×Myc. Cells were harvested 48 h after transfection and homogenized in iso-osmotic buffer. A PNS was obtained and separated in a self-forming Percoll® density gradient (17% Percoll® starting concentration). Activities of the marker enzymes β-hexosaminidase (lysosome) and alkaline phosphatase (plasma membrane) were determined in each fraction. Furthermore, equal volumes of each fraction were subjected to SDS/PAGE and Western blotting in order to assess the distribution of overexpressed DIRC2 by detection of the triple Myc tag or its N-terminus, the lysosomal protease cathepsin D (CD) and the ER marker PDI. Bands representing unprocessed or proteolytically cleaved (N- or C-terminal fragments respectively) DIRC2 are indicated by closed and open arrowheads respectively. The asterisk marks a band observed at varying intensity upon overexpression of DIRC2 and detection with the N-terminal antibody [also in (**B**) top panel, lane 3]. The apparent molecular mass is comparable with the N-terminal fragment after deglycosylation. However, the exact nature and origin of this band are currently unclear. The molecular mass in kDa is indicated on the right-hand side. IP, immunoprecipitation.

proteolytically processed similar to wild-type DIRC2 (Figure 3B). As expected, no molecular-mass-shift of full-length DIRC2-N209A or its N-terminal fragment was detectable upon PNGase F treatment, confirming that DIRC2 carries N-glycans at Asn^{209} and that no further N-glycosylation sites are in use. The observed molecular-mass-shift upon deglycosylation seems remarkably pronounced considering that it was caused by one N-glycosylation site only, indicating that the carbohydrate chain attached to this site exhibits considerable length and/or degree of branching.

Proteolytic processing of DIRC2 was further corroborated by pulse–chase analysis of metabolically labelled HeLa cells transiently expressing DIRC2–3×Myc (Figure 3C, left-hand panel) or the glycosylation mutant DIRC2-N209A–3×Myc (Figure 3C, right-hand panel). Cells were pulse-labelled for 2.5 h and then analysed after chase periods of 0, 3, 11 and 19 h. Whereas the amount of full-length DIRC2 (Figure 3C, closed arrowhead) constantly declined after the end of labelling, the intensity of the C-terminal fragment (Figure 3C, open arrowhead) that is already present in significant amounts at the end of the labelling period (0 h) slightly increased further during the chase period up to 11 h. However after a chase time of 19 h, both full-length and processed DIRC2 seem to be decreased, presumably indicating regular turnover of this protein. It is conceivable that this degradation of DIRC2 also takes place in lysosomal compartments. However, this has not yet been investigated.

Under steady-state conditions, only small amounts of full-length DIRC2 are observed in overexpressing cells. The subcellular distribution of full-length (closed arrowhead) and processed (open arrowhead) DIRC2 was experimentally studied by subcellular fractionation of DIRC2-expressing HeLa cells (Figure 3E). The N- and C-terminal fragments of DIRC2 were detected almost exclusively in fractions 12–14, co-sedimenting with lysosomes, as revealed by the distribution of β-hexosaminidase activity and cathepsin D, confirming previous findings from immunofluorescence. In contrast, the unprocessed precursor represented by two bands at approximately 55 kDa was recovered primarily in fractions 6 and 7 where also the bulk of the ER was localized, as indicated by the ER-marker protein PDI. Only minor amounts of full-length DIRC2 were present in the lysosome-enriched fractions of the gradient. The double band obtained for the DIRC2 precursor most probably represents the ER-form with immature glycosylation and the Golgi-form after completed processing of the oligosaccharide side chains. The band marked with an asterisk on the anti-DIRC2 blot was infrequently observed at variable intensities upon overexpression of DIRC2 and detection with the N-terminal antibody (Figure 3B, top panel, lane 3). The apparent molecular mass was comparable with the N-terminal fragment after deglycosylation. This fragment seems to have a subcellular distribution distinct from that of the C-terminal and glycosylated N-terminal fragment. However, the exact nature and origin of this band are currently unclear.

One central questi[10] is the site of proteolysis within the DIRC2 protein. The apparent molecular masses of 20 kDa of the N-terminal fragment (without N-glycans) and 25 kDa of the C-terminal fragment (Figure 3B) suggested a slightly asymmetric cleavage. Two internal HA tags were inserted after amino acids 214 and 261 (DIRC2-HA214–3×Myc and DIRC2-HA261–3×Myc) respectively, which are located within the intralysosomal loop 5 and the cytosolic loop 6 respectively according to the predicted topology. Specific detection of the C-terminus was ensured by a C-terminally appended triple Myc tag (Figure 3D). Western blot analysis of these DIRC2 variants with anti-DIRC2, anti-Myc and anti-HA antibodies for the specific detection of the N- and C-terminal fragments, as well as the identification of the respective fragment carrying the HA tag, was performed. The band patterns obtained with anti-DIRC2 and anti-Myc antibodies (Figure 3D, middle and right-hand panels) were similar to that of wild-type DIRC2 (Figure 3B), indicating that proteolytic processing of DIRC2 was not impaired by the inserted HA tags. Conspicuously, the band of the C-terminal fragment derived from DIRC2-HA261, as detected by the anti-Myc antibody, exhibited a slightly higher molecular mass than that of DIRC2-HA214, suggesting that the HA tag inserted at position 261 was retained in the C-terminal fragment after cleavage, in contrast with that introduced at position 214. This was confirmed by detection with an anti-HA antibody which recognized full-length DIRC2-HA261 (closed arrowhead) and the processed fragment (open arrowhead), which corresponded exactly to the band detected with the anti-Myc antibody in terms of appearance and molecular mass.

In contrast, bands obtained for DIRC2-HA214 with the anti-HA antibody seem to represent full-length protein and N-terminal fragment (Figure 3B, left-hand panel). However, the signal obtained for the processed form was of rather low intensity as compared with the full-length protein. This seems surprising, since the N-terminal DIRC2 antibody mainly detected the fragment and not the full-length form (Figure 3B, middle panel). A possible explanation might be that the internal HA epitope can be more efficiently accessed by the HA antibody in the full-length form than in the processed protein, leading to an under-representation of the fragment on the Western blot. Furthermore, it is conceivable that the HA tag, although upon proteolysis initially retained within the N-terminal fragment, as suggested by the band pattern with the anti-HA antibody, is not stable in the lysosomal lumen where it would be localized according to the assumed topology of DIRC2 (Figure 1B). Apparently, proteolytic cleavage of DIRC2 occurs between amino acids 214 and 261.

Endogenous DIRC2 is present in lysosomes and post-translationally modified in a similar manner to overexpressed DIRC2

Detection of endogenous DIRC2 in different samples of human and murine origi[11] was attempted. Owing to the high degree of conservation, cross-reactivity of the antiserum with mouse DIRC2 was expected. In total lysates of HeLa cells, weak signals for endogenous DIRC2 were obtained (Figure 4A) accompanied by a variety of non-specific bands unrelated to DIRC2, presumably due to the low abundance of the protein. The specificity of the bands was validated by performing siRNA-mediated knockdown of DIRC2. The effectiveness of the siRNA was also confirmed at the transcript level (Supplementary Figure S1 at http://www.BiochemJ.org/bj/439/bj4390113add.htm). Endogenous DIRC2 in HeLa cell lysates appeared as a heterogenous cluster of bands at approximately 35 kDa, similar in appearance and electrophoretic mobility to the N-terminal fragment of overexpressed DIRC2 (Figure 3B).

In comparison, detection of DIRC2 was greatly facilitated in lysosome-enriched preparations from human placenta and mouse liver (Figure 4B). After deg[9]cosylation, in both materials a single immunoreactive band with an apparent molecular mass of approximately 20 kDa was observed, indicating that endogenous DIRC2 is present in proteolytically processed form in different tissues and species. However, the differences in band patterns observed for DIRC2 in non-deglycosylated samples (Figure 4B) may indicate tissue- and/or species-specific differences regarding glycosylation. Lysosomal residence of endogenous murine DIRC2 could be substantiated by its

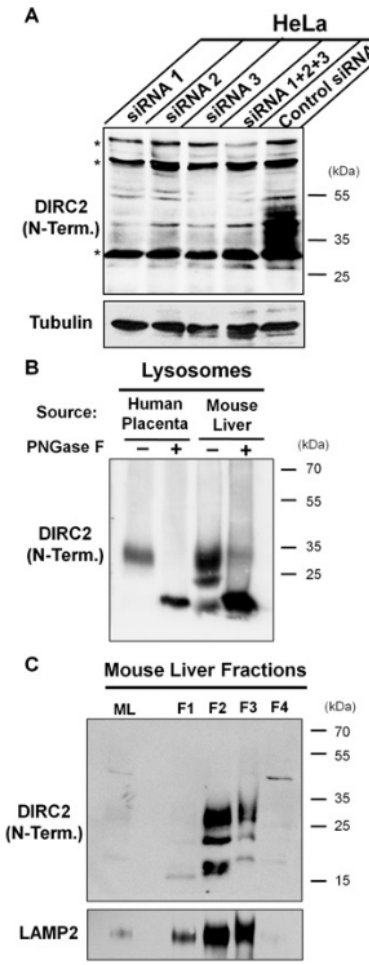

Figure 4 Endogenous DIRC2 is modified and processed in a similar way as overexpressed DIRC2

(**A**) HeLa cells were transiently transfected with three different siRNAs directed against DIRC2 separately or in combination (siRNA 1 + 2 + 3) or a non-targeting control siRNA. Cells were harvested 48 h after transfection and aliquots of total lysates (40 μg of protein) were analysed for the expression level of endogenous DIRC2 protein by Western blotting using the specific DIRC2 antiserum generated against a synthetic peptide derived from the N-terminus of DIRC2. Non-specific bands are indicated by asterisks. (**B**) Aliquots (25 μg of protein) of a lysosomal membrane preparation obtained from human placenta, as well as a lysosomal fraction from mouse liver (Tritosomes) were incubated either in the absence (–) or presence (+) of PNGase F. Samples were resolved by SDS/PAGE and transferred on to nitrocellulose. Membranes were probed with the anti-DIRC2 antibody. (**C**) Endogenous DIRC2 co-sediments with lysosomal membranes as indicated by the lysosomal membrane protein LAMP2. Livers from Triton WR1339-injected mice were homogenized. A lysosome-enriched sediment (ML) was obtained by differential centrifugation and further separated by sucrose-density gradient centrifugation. After centrifugation four different fractions (F1–F4) were collected from top to bottom. Equal aliquots (10 μg of protein) of the ML sediment and of the final gradient fractions F1–F4 were separated by SDS/PAGE and analysed for the presence of DIRC2 and LAMP2 using the anti-DIRC2 antibody described above and a monoclonal anti-LAMP2 antibody (ABL93). The molecular mass in kDa is indicated on the right-hand side.

co-sedimentation with lysosomes (LAMP2) in fraction F2 of the sucrose-density gradient employed for isolation of tritosomes from a crude organellar concentrate 'ML' (Figure 4C).

Proteolytic processing of DIRC2 occurs in lysosomes

The rapid processing observed in the pulse–chase experiment (Figure 3C) could indicate that proteolytic cleavage of DIRC2 occurs early in the biosynthetic pathway. In order to test this hypothesis, the effect of ER retention of DIRC2 was evaluated (Figure 5A) which was achieved by two different approaches. In the first experiment, the fungal metabolite Brefeldin A reversibly interfering with anterograde transport from the ER to the Golgi apparatus [25] was applied to HeLa cells transiently expressing DIRC2–3×Myc. In a second experiment, an established arginine-based ER-retention motif was fused to the C-terminus of the triple Myc tag in DIRC2–3×Myc. Both strategies resulted in ER localization of DIRC2 (Figure 5B and results not shown). No C-terminal fragment and proteolysis of DIRC2 was observed in Brefeldin-A-treated cells transfected with wild-type DIRC2, or in untreated HeLa cells expressing the DIRC2 ER-retention construct. The slightly faster migration of ER-retained full-length DIRC2 in comparison with the wild-type precursor in untreated cells is most likely to be caused by the absence of post-ER oligosaccharide processing. Apparently, proteolytic cleavage of DIRC2 is not taking place in the ER, but further downstream in the Golgi apparatus, endosomes or at its final destination, the lysosome.

In the latter case, misrouting DIRC2 from its final lysosomal destination should inhibit proteolysis. As a preliminary step to test this hypothesis, we characterized the determinants required for lysosomal sorting of DIRC2. Deletion of the C-terminal tail [DIRC2-(Δ464–478)] did not alter lysosomal targeting of overexpressed DIRC2 (results not shown). Therefore the contribution of the putative N-terminal dileucine motif was tested by generating a DIRC2-LL14/15AA–3×Myc (DIRC2-LL/AA) construct in which the critical leucine residues of the putative motif were replaced by alanine residues. In transiently transfected HeLa cells, major portions of this DIRC2 mutant were observed at the plasma membrane, indicating that lysosomal targeting critically depends on this motif (Figure 5C). Since significant amounts of the dileucine mutant are still found in lysosomal/late endosomal compartments, additional sorting determinants within the DIRC2 sequence may exist, providing partial compensation for the loss of the dileucine motif.

Increased cell-surface expression of DIRC2-LL/AA as compared with wild-type DIRC2 was confirmed biochemically by surface biotinylation using the membrane-impermeable reagent sulfo-NHS-SS-biotin and streptavidin-agarose pull down for the recovery of biotinylated proteins (Figure 5D). Apparently, small amounts of overexpressed wild-type DIRC2 are also present at the cell surface, undetected by immunocytochemistry (DIRC2–3×Myc, lane 'B'). In comparison, an increased amount of the LL/AA mutant was detected in the biotinylated protein fraction, confirming an enhanced degree of surface expression. Interestingly, in total lysates of cells expressing DIRC2-LL/AA (lane 'T') the ratio of the final processed form of DIRC2 to the precursor was shifted strongly to the full-length form as compared with wild-type DIRC2 (DIRC2–3×Myc, lane 'T'), indicating that proteolytis of the dileucine mutant was significantly impaired or slowed down. Since a direct effect of the LL/AA mutation on proteolytic processing seems unlikely, this finding suggests that cleavage of DIRC2 requires delivery to lysosomes. In the small fraction of cell-surface-localized wild-type DIRC2 (DIRC2–3×Myc, lane 'B') the fragment/full-length ratio was shifted to the precursor form in a similar way as was observed for the DIRC2-LL/AA mutant. Therefore it can be concluded that DIRC2 proteolysis takes place in endosomal or lysosomal compartments.

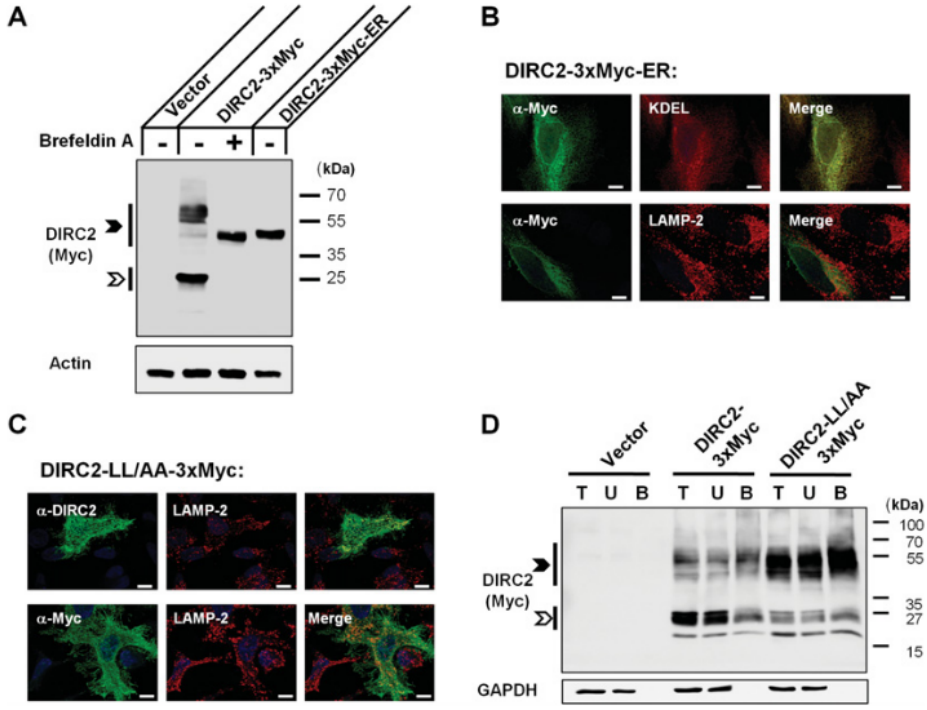

Figure 5 Lysosomal targeting is a prerequisite for proteolytic processing of DIRC2

(**A**) HeLa cells were transiently transfected with wild-type DIRC2–3×Myc-pcDNA3.1/Hygro+ (DIRC2–3×Myc), the ER-retention mutant DIRC2–3×Myc-ER-pcDNA3.1/Hygro+ (DIRC2–3×Myc-ER) or an empty vector. As indicated, Brefeldin A (5 μg/ml final concentration) or an equivalent volume of solvent (methanol) was added to the medium 6 h post-transfection. Cells were harvested after additional 10 h of incubation. Aliquots of total lysates (15 μg per lane) were analysed by Western blotting for full-length (closed arrowhead) and processed (open arrowhead) forms of DIRC2 using an anti-Myc antibody detecting the C-terminally appended epitope tag. The C-terminal fragment of DIRC2 was not detected upon Brefeldin A treatment of cells transfected with wild-type DIRC2 or upon transfection of the ER-retention mutant. (**B**) Subcellular localization of the ER-retention mutant DIRC2–3×Myc-ER in the ER was confirmed in transiently transfected HeLa cells by indirect immunofluorescence. Cells were fixed 24 h after transfection and DIRC2 was visualized with an anti-Myc antibody in combination with anti-KDEL (ER) or anti-LAMP2 (lysosomes/late endosomes) antibodies. (**C**) Disruption of the N-terminal dileucine motif LL14/15AA impairs lysosomal targeting of DIRC2 and redirects DIRC2 to the plasma membrane. The dileucine mutant DIRC2-LL/AA–3×Myc was transiently expressed in HeLa cells. Cells were fixed 24 h after transfection and the DIRC2 mutant was localized using anti-DIRC2 and anti-Myc antibodies detecting the N- and C-terminus respectively. Co-staining with anti-LAMP2 was performed in order to visualize lysosomal compartments. (**D**) Increased plasma membrane localization of the dileucine mutant DIRC2-LL/AA–3×Myc was confirmed biochemically. HeLa cells transiently transfected with wild-type DIRC2–3×Myc, the dileucine mutant DIRC2-LL/AA–3×Myc or empty vector were treated with the membrane-impermeable reagent sulfo-NHS-SS-biotin for specific biotinylation of cell-surface proteins. From total lysates, biotinylated proteins were recovered by pull down with streptavidin-agarose and eluted into SDS/PAGE sample buffer. Aliquots of total lysates (total, T), streptavidin pull down supernatants (unbound, U) and of biotinylated proteins (bound, B) were analysed by Western blotting. The analysed aliquots of the streptavidin-bound material (B) was derived from a 15-fold higher amount of material as compared with the loaded aliquots of starting material (T) and unbound protein (U). Full-length and processed DIRC2 was detected with an anti-Myc antibody. Closed and open arrowheads mark the positions of full-length DIRC2 and the C-terminal fragment respectively. The absence of the cytosolic protein GAPDH in the bound fraction (B) indicates specificity of the performed biotinylation for cell-surface proteins. In (**B**) and (**C**) scale bars represent 10 μM. For Western blots, the molecular mass in kDa is indicated on the right-hand side.

Inhibitory profiling indicates the involvement of lysosomal thiol proteases in proteolysis of DIRC2

In order to identify the protease(s) involved in cleaving DIRC2, modulation of this process by various inhibitors was analysed in transiently transfected HeLa cells. Inhibition of lysosomal acidification by NH_4Cl globally impairs lysosomal function, degradation and proteolytic activity [26]. In cells incubated in the presence of NH_4Cl, no C-terminal fragment of DIRC2 was detected (Figure 6A), substantiating the involvement of lysosomal proteases. Whereas pepstatin A, an inhibitor of aspartic acid proteases such as cathepsin D, showed no effect on DIRC2 processing (Figure 6A), leupeptin prevented generation of the DIRC2 C-terminal fragment in a similar manner to NH_4Cl. Leupeptin is a well-characterized broad spectrum inhibitor of various serine and cysteine proteinases. In lysosomes, several members of the cathepsin protease family are sensitive to leupeptin, among them the thiol proteases cathepsin B [27] and L [28].

For further refinement, the more specific inhibitors E-64, CA-074-Me and Z-FY-CHO were applied in the same experimental setup (Figure 6B). All three compounds completely blocked DIRC2 proteolysis. In contrast with leupeptin, the action of E-64 is restricted to thiol proteases without effecting serine proteinases [29]. Among lysosomal cysteine proteases, the two cathepsins B and L are among the most widely expressed [30] and were therefore considered as possible candidates.

Whereas Z-FY-CHO specifically inhibits cathepsin L [31], CA-074 Me, although initially introduced as a cathepsin B-specific inhibitor, shows overlapping effects on cathepsin B and L if applied to living cells [32]. Both inhibitors were found to be equally effective as leupeptin and E-64 in preventing DIRC2 proteolysis (Figures 6A and 6B), strongly suggesting a critical involvement of cathepsin L. However, based on the experimental data described, an additional role for cathepsin B cannot fully be excluded owing to the overlapping specificities of the inhibitors used.

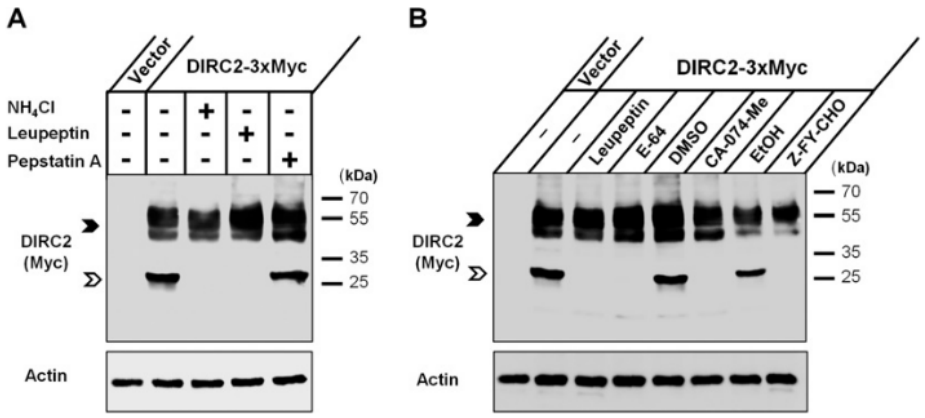

Figure 6 Inhibitory profiling of DIRC2 proteolysis

HeLa cells were transiently transfected with DIRC2–3×Myc-pcDNA3.1/Hygro+ (DIRC2–3×Myc). In order to identify the protease(s) mediating DIRC2 processing, the following inhibitors of lysosomal proteases were added to the cells 6 h post-transfection with the indicated final concentrations in the medium: NH_4Cl (25 mM), leupeptin (100 μM), pepstatin A (1 μg/ml), E-64 (40 μM), CA-074-Me (40 μM) and Z-FY-CHO (40 μM). Solvent controls were performed with equivalent volumes of DMSO and ethanol (EtOH) as indicated. Cells were harvested 16 h post-transfection after being cultured for 10 h in the presence of the inhibitors. Total lysates were separated by SDS/PAGE (15 μg of protein per lane) and transferred on to nitrocellulose. Membranes were probed with an anti-Myc antibody detecting full-length (closed arrowhead) DIRC2 and the C-terminal fragment (open arrowhead). In a first experiment, inhibitors with broad specificity (**A**) were tested. In the presence of NH_4Cl and leupeptin, no C-terminal fragment of DIRC2 was observed, suggesting the involvement of lysosomal thiol proteinases. In a second approach this was corroborated (**B**) by using the thiol proteinase inhibitor E-64, the cathepsin B inhibitor CA-074-Me and the cathepsin L inhibitor Z-FY-CHO, which inhibited DIRC2 proteolysis equally effectively as leupeptin and NH_4Cl. The molecular mass in kDa is indicated on the right-hand side.

Cathepsin L, but not cathepsin B, is critically involved in processing of DIRC2

In order to scrutinize the involvement of cathepsin L and B in DIRC2 proteolysis, the processing of overexpressed DIRC2–3×Myc was examined in different protease-deficient MEF cell lines (Figure 7A and Supplementary Figures S2 and S3 at http://www.BiochemJ.org/bj/439/bj4390113add.htm). No C-terminal fragment of DIRC2 (open arrowhead) was observed in cathepsin L-deficient ($CtsL^{-/-}$) or cathepsin B and L double-deficient ($CtsBL^{-/-}$) cells, whereas proteolytic processing in cathepsin B-deficient ($CtsB^{-/-}$), as well as cathepsin D-deficient ($CtsD^{-/-}$) MEFs was preserved (Figure 7A). Since delivery of DIRC2 to lysosomes is a prerequisite for proteolytic processing in HeLa cells, lysosomal localization of overexpressed DIRC2 was confirmed in all MEF cell lines analysed (Supplementary Figure S2). In agreement with the inhibitor studies, these findings corroborated a critical role for cathepsin L in the processing of DIRC2. Cathepsin B, which is endogenously expressed in MEFs [33], is obviously unable to compensate for the deficiency of cathepsin L. Furthermore, the loss of cathepsin B does not alter processing of DIRC2 in cathepsin B-deficient cells. Therefore a role for cathepsin B in proteolysis of DIRC2 seems unlikely.

For excluding overexpression artefacts, endogenous DIRC2 was analysed in total cellular membranes from cathepsin L-deficient and wild-type MEFs that had been depleted of cytosolic and membrane-associated proteins by sodium carbonate treatment for enhancing detection of DIRC2 (Figure 7B). In cathepsin L-deficient cells, DIRC2 was present exclusively as an unprocessed precursor with an apparent molecular mass of approximately 55 kDa (Figure 7B, closed arrowhead), whereas in wild-type cells the bulk of endogenous DIRC2 was proteolysed, confirming the results obtained for overexpressed DIRC2. In addition, tritosomes isolated from livers of cathepsin L-deficient and wild-type mice were analysed by Western blotting for DIRC2 (Figure 7C). Surprisingly, cathepsin L deficiency only exhibits a minor effect on DIRC2 proteolysis in liver. This is in contrast with the situation in fibroblasts shown in Figure 7(B), where virtually no fragmented DIRC2 was detected. In cathepsin L-deficient liver lysosomes, the bulk of DIRC2 was present in a proteolysed form. Apparently, in liver the function of cathepsin L can be compensated for by other proteases to a significant degree. However, the amount of detectable full-length precursor appeared to be slightly increased in cathepsin L-deficient tritosomes (Figure 7C, closed arrowhead).

Full-length DIRC2 is an electrogenic transporter

In order to investigate the presumed transport function of DIRC2, we used the LL14/15AA mutant, since several lysosomal transporters have been functionally characterized in whole cells using recombinant proteins ectopically expressed at the plasma membrane [34–36]. The advantage of this approach is to replace a poorly tractable lysosomal efflux by a simple whole-cell influx. As preliminary attempts using candidate substrates were unsuccessful, we used a generic approach based, on one hand, on the application of a complex mixture of (unlabelled) metabolites to avoid *a priori* hypotheses on the substrate and, on the other hand, on electrophysiological detection of transport activity.

For this purpose, DIRC2 constructs bearing a C-terminal EGFP tag were overexpressed in *Xenopus* oocytes, a popular model for electrophysiological analysis of transporters. Epifluorescence microscopy and surface biotinylation analyses of the cRNA-injected oocytes showed that, whereas the wild-type protein was localized predominantly intracellularly, a substantial amount of LL14/15AA mutant was misrouted to the oocyte surface (Figures 8A and 8B), in agreement with the role of the dileucine motif in HeLa cells (Figures 5C and 5D). Western blot analysis indicated that wild-type and LL/AA DIRC2–EGFP were expressed at similar levels in oocytes. However, in contrast with their fate in mammalian cells, none of these DIRC2 fusion proteins was detectably in a proteolytically cleaved form. In particular, a ~70 kDa DIRC2–EGFP band was selectively expressed at the

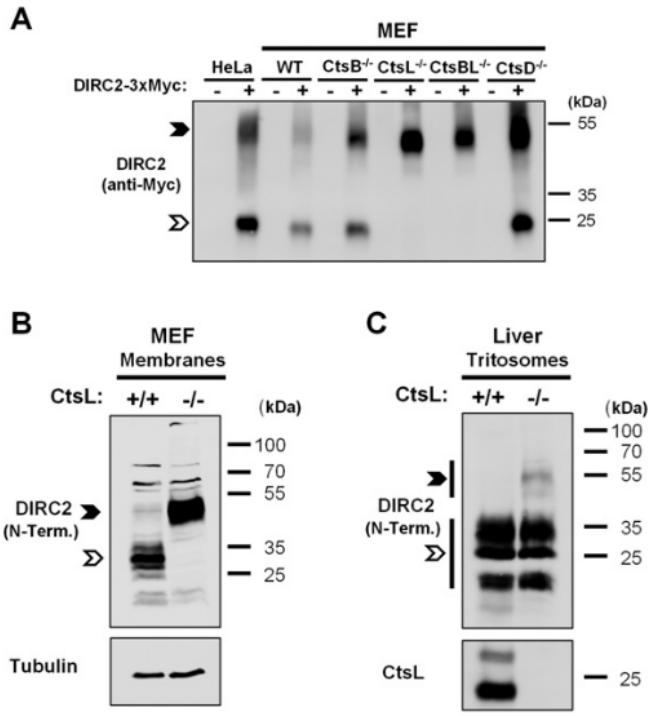

Figure 7 Cathepsin L is critically involved in proteolytic processing of DIRC2

(**A**) HeLa cells as well as MEFs derived from wild-type mice (WT) or mouse strains deficient in one or more lysosomal proteases (cathepsin B, CtsB$^{-/-}$; cathepsin L, CtsL$^{-/-}$; cathepsin B and L, CtsBL$^{-/-}$; cathepsin D, CtsD$^{-/-}$) were transiently transfected with DIRC2–3×Myc-pcDNA3.1/Hygro + (+) or empty vector (−). Cells were harvested 48 h after transfection and aliquots of total lysates (20 μg of protein) were subjected to SDS/PAGE and Western blotting. Overexpressed DIRC2 was detected with an anti-Myc antibody. In CtsL$^{-/-}$ and CtsBL$^{-/-}$ cells, DIRC2 was not proteolytically processed, which was indicated by the absence of a C-terminal fragment. (**B**) CtsL$^{-/-}$ MEFs were mechanically disrupted and a PNS was prepared. Total cellular membranes were sedimented at 50 000 rev./min for 1 h and washed with sodium carbonate in order to remove membrane-associated proteins. Aliquots of carbonate-washed membranes (50 μg of protein) were separated by SDS/PAGE and transferred on to nitrocellulose. Membranes were probed with anti-DIRC2 antibody directed against an N-terminal epitope and anti-tubulin as a control. (**C**) Enriched lysosomes (Tritosomes) from livers of WT (+/+) and cathepsin L-deficient mice (−/−) were subjected to SDS/PAGE and Western blot analysis (25 μg of protein per lane). DIRC2 and cathepsin L were detected with appropriate antibodies. Positions of full-length and the proteolytically processed (N- or C-terminal fragment respectively) forms of DIRC2 are indicated by closed and open arrowheads respectively. The molecular mass in kDa is indicated on the right-hand side.

oocyte surface (Figure 8B), thus limiting our functional analysis to the unprocessed protein.

To test whether full-length DIRC2 transports small molecules, oocytes were recorded by two-electrode voltage clamp. A metabolite mixture (BYE) was applied to clamped oocytes in an acidic extracellular medium (pH 5.0), a condition mimicking the natural environment of DIRC2 in the lysosome (the extracellular medium being topologically equivalent to the lysosomal lumen). Application of BYE immediately induced a small, but significant, outward current in DIRC2-LL/AA–EGFP oocytes ($+28.7 \pm 4.2$ nA, $n = 9$), but not in naïve (water-injected) or wild-type DIRC2–EGFP oocytes (Figures 8C and 8D), thus showing that this current is associated with the presence of DIRC2 at the oocyte surface. Upon prolonged application of BYE, the current did not reach a steady state, but instead continuingly decreased towards negative values. However, this behaviour was observed in all oocytes irrespective of the surface expression of DIRC2 (Figure 8C) and may presumably result from the uptake, metabolization and subsequent electrogenic catabolite efflux of some BYE components through endogenous oocyte transporters. Taken together, these data indicate that full-length DIRC2 functions as an electrogenic transporter. Moreover, the outward direction of the DIRC2-LL/AA-associated current suggests that the as yet unknown DIRC2 substrate present in BYE is anionic, or that it is co-transported with lysosomal anions or exchanged for cytosolic cations (more complex ion stoichiometries, however, cannot be excluded).

DISCUSSION

DIRC2 is a novel lysosomal protein

In the present study we have demonstrated in different experimental setups employing immunocytochemistry and subcellular fractionation that overexpressed as well as endogenous DIRC2 resides in lysosomal membranes. This had been suggested by its previous identification in a comparative proteomic analysis of human placental lysosomal membranes [4].

Similar to many other lysosomal proteins, DIRC2 was found to be a glycoprotein. N-glycosylation of Asn^{209} could be experimentally confirmed. According to the predicted topology this residue directly borders on a transmembrane segment. This is uncommon for sugar acceptor sites which usually require a minimum distance of 12–14 residues to the membrane in order to be utilised by the glycosylation machinery [37]. Possibly, the borders of the transmembrane segments within the depicted DIRC2 topology have not been predicted correctly in all cases. The large size of the attached carbohydrate moiety suggests

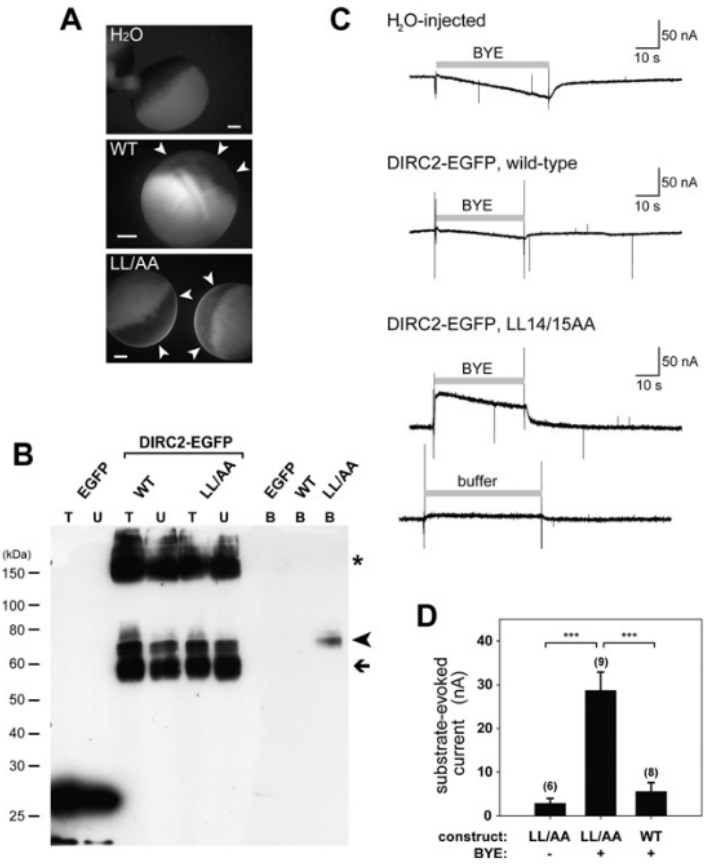

Figure 8 DIRC2 is an electrogenic transporter

Xenopus oocytes, previously injected with water or cRNAs coding for wild-type or LL14/15AA DIRC2–EGFP, were analysed by fluorescence microscopy and by two-electrode voltage clamp. (**A**) Epifluorescence micrographs show that DIRC2-LL/AA–EGFP, but not the wild-type protein, is expressed at or near the oocyte surface (arrowheads). Scale bar, 0.2 mm. (**B**) Surface biotinylation analysis of DIRC2 oocytes. Pools of five oocytes expressing WT or mutant DIRC2–EGFP, or EGFP as a negative control, were biotinylated with an impermeant reagent. After solubilization and fractionation using streptavidin-agarose, equal amounts of total lysate (T) and streptavidin-unbound material (U), and a 10-fold higher amount of streptavidin-bound material (B), were analysed by immunoblotting with anti-GFP antibodies. The absence of streptavidin-bound EGFP in the negative control confirms that only surface proteins were biotinylated. A GFP-tagged 70 kDa band is selectively expressed at the surface of DIRC2-LL/AA–EGFP oocytes (arrowhead). DIRC2 aggregates (asterisk) and a 58 kDa band (arrow), presumably reflecting immature glycosylation, are also present within the cells. (**C**) Representative current traces acquired at pH 5.0 and −40 mV are shown. Application of BYE (grey bar) selectively evokes an outward current in the DIRC2-LL/AA–EGFP oocyte. This response was suppressed when BYE was omitted from the substrate application channel (bottom trace recorded from the same oocyte). (**D**) Evoked currents were measured 1 s after the onset of substrate (BYE) application over a time window of 0.5 s. Results are mean ± S.E.M. values from the indicated numbers of wild-type or LL/AA DIRC2–EGFP oocytes. $^{***}P < 0.0005$.

an unusual N-glycan of the polylactosamine type, as shown previously to be present on LAMP proteins [38].

The identified targeting motif perfectly fits the consensus sequence of canonical dileucine motifs [DE]XXXL[LI] [39]. In the case of DIRC2, 37 residues separate the dileucine from the first putative transmembrane segment. Interestingly, the majority of dileucine signals identified as sorting determinants in late endosomal/lysosomal proteins are positioned in closer proximity to the adjacent transmembrane segment [39]. In some proteins, lipid modifications have been reported to alter the accessibility and function of sorting motifs, e.g. in the cation-dependent mannose 6-phosphate receptor [40]. Using bioinformatic analysis (http://www.expasy.org/myristoylator), myristoylation of the glycine residue at position 2 of the DIRC2 sequence is likely to occur after removal of the initiating methionine residue. This would attach the N-terminus to the membrane and, thereby, also bring the dileucine motif in closer vicinity to the membrane. However, the presence and functional relevance of this post-translational modification may still need experimental confirmation.

Proteolytic processing of DIRC2

The present results demonstrate that DIRC2 is subjected to limited proteolysis in lysosomal compartments. Lysosomes are the site of degradation of many plasma membrane proteins, among these are also many transport proteins which are delivered there after endocytotic internalisation [41]. Therefore lysosomal proteolysis of a transport protein may in principle also represent the initiation of degradation of a cargo protein that is not primarily localized in lysosomes. However, overexpressed as well as endogenous DIRC2 was found to be stably associated with lysosomes under steady-state conditions. Only very minor amounts of overexpressed wild-type DIRC2 were observed at the plasma membrane, which was only detectable by surface

biotinylation and not by *in situ* immunolocalization. The proteolytic fragments observed represent very distinct protein species and exhibit considerable stability in the lysosome, which seems unlikely if these were degradation intermediates. Finally, endogenous DIRC2 is observed nearly exclusively in its proteolysed form in different cell types and tissues. Proteolytic processing of lysosomal hydrolases has been extensively studied. In contrast, only few examples of lysosomal membrane proteins undergoing proteolytic processing have been reported so far, such as HSGNAT (heparin-α-glucosaminide *N*-acetyltransferase) [42], mucolipin-1 [43] and TLR9 (Toll-like receptor 9) [44].

The exact cleavage site within DIRC2 has not yet been identified. The analysis of DIRC2 constructs containing internal HA tags (DIRC2-HA214–3×Myc and DIRC2-HA261–3×Myc) has suggested that cleavage occurs between amino acid residues 214 and 261. The requirement of lysosomal targeting for processing to occur, as well as the dependence of the process on lysosomal acidification, strongly suggest that the cleavage site is localized within a loop of DIRC2 exposed towards the lysosomal lumen. Taken together, based on the results of the present study, cleavage of DIRC2 between amino acid 214 and the subsequent transmembrane segment which starts at residue 230 according to prediction, has to be assumed.

The role of cathepsin L

The experiments performed indicate very consistently a crucial role for cathepsin L and its proteolytic activity for DIRC2 processing. It is tempting to assume the most obvious connection which would be direct proteolytic action of cathepsin L on DIRC2, as was shown for TLR9 [44]. However, based on the findings of the present study, indirect effects from cathepin L on DIRC2 cleavage cannot be excluded. The network of lysosomal proteases is closely interwoven with regard to their action and especially their activation [45]. It is conceivable that cathepsin L critically contributes to the activation of another protease that then cleaves DIRC2.

Although traditionally lysosomal proteases were believed to perform unspecific bulk proteolysis, specific tasks of cysteine cathepsins have been characterized [46,47]. Non-redundant functions of cathepsin L are indicated by the specific phenotype of cathepsin L-deficient (CtsL$^{-/-}$) mice [15], which is characterized by dilated cadiomyopathy [48] as well as epidermal hyperproliferation in conjunction with retardation of hair follicle morphogenesis and alterations of the hair cycle [15,46]. The observation that DIRC2 processing is not impaired in liver cells of cathepsin L-deficient mice demonstrates that other proteases, that are either not present or not active in MEFs, can in principle compensate for the loss of cathepsin L. Functional redundancy and overlapping specificities among lysosomal proteases are a known phenomenon, illustrated, for example, by the absence of any spontaneous phenotype in cathepsin B-deficient mice [46]. However, the contribution of individual cathepsins to the cleavage of particular substrates can vary in a tissue- and cell-type-specific manner. This is exemplified by the processing/degradation of the invariant chain (Ii) that functions as a chaperone for MHCII complexes. Whereas cathepsin L significantly participates in Ii processing in the thymus, cathepsin S and F seem to perform this function in peripheral antigen-presenting cells such as dendritic cells, B-lymphocytes and macrophages. Consequently, no impairment of Ii processing is observed in these cell types in cathepsin L-deficient mice [46]. In a similar way, the processing of DIRC2 in different tissues may be catalysed by distinct proteases and further studies may be required to dissect this.

DIRC2 is an electrogenic metabolite transporter

To test whether DIRC2 may export hydrolysis products from the lysosome, we expressed its dileucine-sorting mutant at the surface of *Xenopus* oocytes and, using electrophysiological recording, examined indirectly whether these oocytes can take up metabolites through a transport process equivalent to lysosomal efflux. The existence of an electric response evoked by a metabolite mixture selectively associated with the presence of DIRC2 at the oocyte surface strongly supports this hypothesis. Although our results do not formally exclude the possibility that DIRC2 can also operate in the reverse direction to import metabolites into the lysosome, the most likely interpretation is that DIRC2 is a lysosomal exporter, which acts downstream of some lysosomal enzymes to recycle their products into cellular metabolism, as do several lysosomal transporters characterized thus far [34–36]. Further fractionation of the BYE used in these experiments may help to identify the nature of DIRC2 substrates and the associated catabolic pathway(s). The fact that an outward current was detected is somewhat surprising since lysosomal transporters are generally coupled to an efflux of protons, which would generate on the contrary an inward current. Possible explanations could be that DIRC2 substrates are anionic, or that their export is driven by cytosolic cations or lysosomal anions. In the latter case, an attractive possibility would be that DIRC2 activity is driven by chloride ions, which have been shown recently to accumulate in lysosomes [49]. Although this lysosomal chloride accumulation has been implied in neuron survival and, to some extent, osteoclast function, its precise molecular role remains elusive [49].

The meaning of proteolytic processing with regard to the function of DIRC2 is currently unknown since the discussed transport activity has been detected for the unprocessed precursor. However, endogenous DIRC2 was found to be present almost completely in proteolysed form. According to our knowledge, DIRC2 is the first example of a MFS protein undergoing proteolytic processing and therefore the general question arises as to whether MFS proteins may exert transport activity after being cleaved in two fragments. For only a few MFS members structural data is available. High resolution structures for the lactose permease (LacY) [7] and the glycerol 3-phosphate transporter (GlpT) [8] from *Escherichia coli*, as well as a low-resolution structure of a bacterial oxalate transporter (OxlT) have been obtained [9]. These structures indicate that MFS proteins comprise two symmetrically arranged domains each consisting of six densely packed transmembrane helices and five short connecting loops. The domains surrounding a pore are held together by a longer central loop linking helices VI and VII [5]. We assume that this arrangement is true also for DIRC2 (Figure 1). On this basis, one may have expected that a proteolytic cleavage maintains the symmetry and results in two equally sized fragments with each comprising six transmembrane segments. However, the present findings suggest proteolytic fragments containing five and seven transmembrane segments respectively.

For the lactose permease (LacY) from *E. coli* it was demonstrated that continuity of the polypeptide chain is not a prerequisite for function. This was revealed by expressing the LacY protein as two non-overlapping fragments and assaying for biological activity. For a variety of different split points that were tested, reconstitution of transport activity could be shown [50]. With regard to DIRC2, these observations indicate that a MFS protein cleaved in two fragments can in principle exert transport activity. Whether this is the case for DIRC2 and in what way its transport activity is modulated by proteolysis, will be subject to further studies, as well as the possible molecular

interaction between the two fragments which would then have to be postulated.

Certainly, the findings in the present study on DIRC2 may pave the way to clarify the possible role for this transporter in the development of cancer. Initially, this was suggested by the identification of a breakpoint within its gene in a chromosomal translocation found in patients suffering from renal cancer. The recent detection of fusion transcripts between DIRC2 and the gene *TIA1* [51] in a prostate cancer cell line suggests that chromosomal rearrangements involving DIRC2 seem not just to be a single finding and that the *DIRC2* gene and protein may deserve further attention.

AUTHOR CONTRIBUTION

Lalu Rudyat Telly Savalas performed most of the experiments in mammalian cells. Bruno Gasnier, Cécile Debacker and Adrien Jézégou contributed the functional and biochemical analysis of DIRC2 in *Xenopus* oocytes. Markus Damme and Torben Lübke performed the isolation of tritosomes from wild-type and cathepsin-deficient mice. Andrej Hasilik and Christian Wrocklage analysed the maturation of DIRC2 by pulse–chase experiments. Thomas Reinheckel provided expertise on cathepsin proteases as well as cathepsin-deficient mice and cell lines. Paul Saftig obtained grant support and contributed to the design of the study. Bernd Schröder designed and supervised the study, and wrote the paper. All authors contributed to the editing of the paper.

ACKNOWLEDGEMENTS

We thank Sebastian Held for excellent technical assistance and M. Hediger for the gift of the pOX(+) plasmid.

FUNDING

This work was supported by the Deutsche Forschungsgemeinschaft (DFG) and the Centre National de la Recherche Scientifique (CNRS). L.R.T.S has received Ph.D. scholarships from the German Academic Exchange Service (DAAD) and the Directorate of Higher Education, Ministry of Education, Republic of Indonesia.

REFERENCES

1 Saftig, P. and Klumperman, J. (2009) Lysosome biogenesis and lysosomal membrane proteins: trafficking meets function. Nat. Rev. Mol. Cell Biol. **10**, 623–635
2 Schröder, B. A., Wrocklage, C., Hasilik, A. and Saftig, P. (2010) The proteome of lysosomes. Proteomics **10**, 4053–4076
3 Sagne, C. and Gasnier, B. (2008) Molecular physiology and pathophysiology of lysosomal membrane transporters. J. Inherit. Metab. Dis. **31**, 258–266
4 Schröder, B., Wrocklage, C., Pan, C., Jager, R., Kösters, B., Schafer, H., Elsasser, H. P., Mann, M. and Hasilik, A. (2007) Integral and associated lysosomal membrane proteins. Traffic **8**, 1676–1686
5 Law, C. J., Maloney, P. C. and Wang, D. N. (2008) Ins and outs of major facilitator superfamily antiporters. Annu. Rev. Microbiol. **62**, 289–305
6 Pao, S. S., Paulsen, I. T. and Saier, Jr, M. H. (1998) Major facilitator superfamily. Microbiol. Mol. Biol. Rev. **62**, 1–34
7 Abramson, J., Smirnova, I., Kasho, V., Verner, G., Kaback, H. R. and Iwata, S. (2003) Structure and mechanism of the lactose permease of *Escherichia coli*. Science **301**, 610–615
8 Huang, Y., Lemieux, M. J., Song, J., Auer, M. and Wang, D. N. (2003) Structure and mechanism of the glycerol 3-phosphate transporter from *Escherichia coli*. Science **301**, 616–620
9 Hirai, T., Heymann, J. A., Shi, D., Sarker, R., Maloney, P. C. and Subramaniam, S. (2002) Three-dimensional structure of a bacterial oxalate transporter. Nat. Struct. Biol. **9**, 597–600
10 Bodmer, D., Eleveld, M., Kater-Baats, E., Janssen, I., Janssen, B., Weterman, M., Schoenmakers, E., Nickerson, M., Linehan, M., Zbar, B. and van Kessel, A. G. (2002) Disruption of a novel MFS transporter gene, DIRC2, by a familial renal cell carcinoma-associated t(2;3)(q35;q21). Hum. Mol. Genet. **11**, 641–649
11 Hentze, M., Hasilik, A. and von Figura, K. (1984) Enhanced degradation of cathepsin D synthesized in the presence of the threonine analog β-hydroxynorvaline. Arch. Biochem. Biophys. **230**, 375–382
12 Diettrich, O., Gallert, F. and Hasilik, A. (1996) Purification of lysosomal membrane proteins from human placenta. Eur. J. Cell Biol. **69**, 99–106
13 Schwappach, B., Zerangue, N., Jan, Y. N. and Jan, L. Y. (2000) Molecular basis for K(ATP) assembly: transmembrane interactions mediate association of a K^+ channel with an ABC transporter. Neuron **26**, 155–167
14 Takanaga, H., Mackenzie, B., Suzuki, Y. and Hediger, M. A. (2005) Identification of mammalian proline transporter SIT1 (SLC6A20) with characteristics of classical system Imino. J. Biol. Chem. **280**, 8974–8984
15 Roth, W., Deussing, J., Botchkarev, V. A., Pauly-Evers, M., Saftig, P., Hafner, A., Schmidt, P., Schmahl, W., Scherer, J., Anton-Lamprecht, I. et al. (2000) Cathepsin L deficiency as molecular defect of furless: hyperproliferation of keratinocytes and pertubation of hair follicle cycling. FASEB J. **14**, 2075–2086
16 Halangk, W., Lerch, M. M., Brandt-Nedelev, B., Roth, W., Ruthenbuerger, M., Reinheckel, T., Domschke, W., Lippert, H., Peters, C. and Deussing, J. (2000) Role of cathepsin B in intracellular trypsinogen activation and the onset of acute pancreatitis. J. Clin. Invest. **106**, 773–781
17 Sevenich, L., Pennacchio, L. A., Peters, C. and Reinheckel, T. (2006) Human cathepsin L rescues the neurodegeneration and lethality in cathepsin B/L double-deficient mice. Biol. Chem. **387**, 885–891
18 Saftig, P., Hetman, M., Schmahl, W., Weber, K., Heine, L., Mossmann, H., Koster, A., Hess, B., Evers, M. and von Figura, K. (1995) Mice deficient for the lysosomal proteinase cathepsin D exhibit progressive atrophy of the intestinal mucosa and profound destruction of lymphoid cells. EMBO J. **14**, 3599–3608
19 Schröder, B., Wrocklage, C., Hasilik, A. and Saftig, P. (2010) Molecular characterisation of 'transmembrane protein 192' (TMEM192), a novel protein of the lysosomal membrane. Biol. Chem. **391**, 695–704
20 Laemmli, U. K. (1970) Cleavage of structural proteins during the assembly of the head of bacteriophage T4. Nature **227**, 680–685
21 Lorkowski, G., Zijderhand-Bleekemolen, J. E., Erdos, E. G., von Figura, K. and Hasilik, A. (1987) Neutral endopeptidase-24.11 (enkephalinase). Biosynthesis and localization in human fibroblasts. Biochem. J. **248**, 345–350
22 Schieweck, O., Damme, M., Schröder, B., Hasilik, A., Schmidt, B. and Lubke, T. (2009) NCU-G1 is a highly glycosylated integral membrane protein of the lysosome. Biochem. J. **422**, 83–90
23 von Figura, K. (1977) Human α-N-acetylglucosaminidase. 1. Purification and properties. Eur. J. Biochem. **80**, 523–533
24 Taute, A., Watzig, K., Simons, B., Lohaus, C., Meyer, H. and Hasilik, A. (2002) Presence of detergent-resistant microdomains in lysosomal membranes. Biochem. Biophys. Res. Commun. **298**, 5–9
25 Pelham, H. R. (1991) Multiple targets for brefeldin A. Cell **67**, 449–451
26 Hasilik, A. and Neufeld, E. F. (1980) Biosynthesis of lysosomal enzymes in fibroblasts. Synthesis as precursors of higher molecular weight. J. Biol. Chem. **255**, 4937–4945
27 Baici, A. and Gyger-Marazzi, M. (1982) The slow, tight-binding inhibition of cathepsin B by leupeptin. A hysteretic effect. Eur. J. Biochem. **129**, 33–41
28 Kirschke, H., Langner, J., Wiederanders, B., Ansorge, S. and Bohley, P. (1977) Cathepsin L. A new proteinase from rat-liver lysosomes. Eur. J. Biochem. **74**, 293–301
29 Barrett, A. J., Kembhavi, A. A., Brown, M. A., Kirschke, H., Knight, C. G., Tamai, M. and Hanada, K. (1982) L-*trans*-Epoxysuccinyl-leucylamido(4-guanidino)butane (E-64) and its analogues as inhibitors of cysteine proteinases including cathepsins B, H and L. Biochem. J. **201**, 189–198
30 Brix, K., Dunkhorst, A., Mayer, K. and Jordans, S. (2008) Cysteine cathepsins: cellular roadmap to different functions. Biochimie **90**, 194–207
31 Woo, J. T., Yamaguchi, K., Hayama, T., Kobori, T., Sigeizumi, S., Sugimoto, K., Kondo, K., Tsuji, T., Ohba, Y., Tagami, K. and Sumitani, K. (1996) Suppressive effect of N-(benzyloxycarbonyl)-L-phenylalanyl-L-tyrosinal on bone resorption *in vitro* and *in vivo*. Eur. J. Pharmacol. **300**, 131–135
32 Montaser, M., Lalmanach, G. and Mach, L. (2002) CA-074, but not its methyl ester CA-074Me, is a selective inhibitor of cathepsin B within living cells. Biol. Chem. **383**, 1305–1308
33 Ebert, D. H., Deussing, J., Peters, C. and Dermody, T. S. (2002) Cathepsin L and cathepsin B mediate reovirus disassembly in murine fibroblast cells. J. Biol. Chem. **277**, 24609–24617
34 Sagne, C., Agulhon, C., Ravassard, P., Darmon, M., Hamon, M., El Mestikawy, S., Gasnier, B. and Giros, B. (2001) Identification and characterization of a lysosomal transporter for small neutral amino acids. Proc. Natl. Acad. Sci. U.S.A. **98**, 7206–7211
35 Kalatzis, V., Cherqui, S., Antignac, C. and Gasnier, B. (2001) Cystinosin, the protein defective in cystinosis, is a H^+-driven lysosomal cystine transporter. EMBO J. **20**, 5940–5949
36 Morin, P., Sagne, C. and Gasnier, B. (2004) Functional characterization of wild-type and mutant human sialin. EMBO J. **23**, 4560–4570
37 Cheung, J. C. and Reithmeier, R. A. (2007) Scanning N-glycosylation mutagenesis of membrane proteins. Methods **41**, 451–459
38 Nabi, I. R. and Dennis, J. W. (1998) The extent of polylactosamine glycosylation of MDCK LAMP-2 is determined by its Golgi residence time. Glycobiology **8**, 947–953

39 Bonifacino, J. S. and Traub, L. M. (2003) Signals for sorting of transmembrane proteins to endosomes and lysosomes. Annu. Rev. Biochem. **72**, 395–447
40 Schweizer, A., Kornfeld, S. and Rohrer, J. (1996) Cysteine34 of the cytoplasmic tail of the cation-dependent mannose 6-phosphate receptor is reversibly palmitoylated and required for normal trafficking and lysosomal enzyme sorting. J. Cell Biol. **132**, 577–584
41 Schulze, H., Kolter, T. and Sandhoff, K. (2009) Principles of lysosomal membrane degradation: cellular topology and biochemistry of lysosomal lipid degradation. Biochim. Biophys. Acta **1793**, 674–683
42 Durand, S., Feldhammer, M., Bonneil, E., Thibault, P. and Pshezhetsky, A. V. (2010) Analysis of the biogenesis of heparan sulfate acetyl-CoA:α-glucosaminide N-acetyltransferase provides insights into the mechanism underlying its complete deficiency in mucopolysaccharidosis IIIC. J. Biol. Chem. **285**, 31233–31242
43 Miedel, M. T., Weixel, K. M., Bruns, J. R., Traub, L. M. and Weisz, O. A. (2006) Posttranslational cleavage and adaptor protein complex-dependent trafficking of mucolipin-1. J. Biol. Chem. **281**, 12751–12759
44 Park, B., Brinkmann, M. M., Spooner, E., Lee, C. C., Kim, Y. M. and Ploegh, H. L. (2008) Proteolytic cleavage in an endolysosomal compartment is required for activation of Toll-like receptor 9. Nat. Immunol. **9**, 1407–1414
45 Ishidoh, K. and Kominami, E. (2002) Processing and activation of lysosomal proteinases. Biol. Chem. **383**, 1827–1831
46 Reinheckel, T., Deussing, J., Roth, W. and Peters, C. (2001) Towards specific functions of lysosomal cysteine peptidases: phenotypes of mice deficient for cathepsin B or cathepsin L. Biol. Chem. **382**, 735–741
47 Reiser, J., Adair, B. and Reinheckel, T. (2010) Specialized roles for cysteine cathepsins in health and disease. J. Clin. Invest. **120**, 3421–3431
48 Stypmann, J., Glaser, K., Roth, W., Tobin, D. J., Petermann, I., Matthias, R., Monnig, G., Haverkamp, W., Breithardt, G., Schmahl, W. et al. (2002) Dilated cardiomyopathy in mice deficient for the lysosomal cysteine peptidase cathepsin L. Proc. Natl. Acad. Sci. U.S.A. **99**, 6234–6239
49 Weinert, S., Jabs, S., Supanchart, C., Schweizer, M., Gimber, N., Richter, M., Rademann, J., Stauber, T., Kornak, U. and Jentsch, T. J. (2010) Lysosomal pathology and osteopetrosis upon loss of H^+-driven lysosomal Cl^- accumulation. Science **328**, 1401–1403
50 Wrubel, W., Stochaj, U., Sonnewald, U., Theres, C. and Ehring, R. (1990) Reconstitution of an active lactose carrier *in vivo* by simultaneous synthesis of two complementary protein fragments. J. Bacteriol. **172**, 5374–5381
51 Maher, C. A., Palanisamy, N., Brenner, J. C., Cao, X., Kalyana-Sundaram, S., Luo, S., Khrebtukova, I., Barrette, T. R., Grasso, C., Yu, J. et al. (2009) Chimeric transcript discovery by paired-end transcriptome sequencing. Proc. Natl. Acad. Sci. U.S.A. **106**, 12353–12358

Received 25 January 2011/6 May 2011; accepted 22 June 2011
Published as BJ Immediate Publication 22 June 2011, doi:10.1042/BJ20110166

Biochem. J. (2011) **439**, 113–128 (Printed in Great Britain) doi:10.1042/BJ20110166

online data

SUPPLEMENTARY ONLINE DATA

Disrupted in renal carcinoma 2 (DIRC2), a novel transporter of the lysosomal membrane, is proteolytically processed by cathepsin L

Lalu Rudyat Telly SAVALAS*[1,2], Bruno GASNIER†[1], Markus DAMME‡, Torben LÜBKE§, Christian WROCKLAGE‖, Cécile DEBACKER†, Adrien JÉZÉGOU†¶, Thomas REINHECKEL**, Andrej HASILIK‖, Paul SAFTIG*[3] and Bernd SCHRÖDER*[3]

*Biochemical Institute, Christian-Albrechts-University, Kiel, Germany, †Université Paris Descartes, Centre National de la Recherche Scientifique, UMR 8192 Paris, France, ‡Department of Biochemistry, University of Bielefeld, Bielefeld, Germany, §Biochemistry II, University of Göttingen, Göttingen, Germany, ‖Institute for Physiological Chemistry, Philipps University, Marburg, Germany, ¶Graduate School ED 419, Université Paris-Sud 11, Kremlin-Bicêtre, France, and **Institute for Molecular Medicine and Cell research and Centre for Biological Signalling Studies (bioss), Albert-Ludwigs-University, Freiburg, Germany

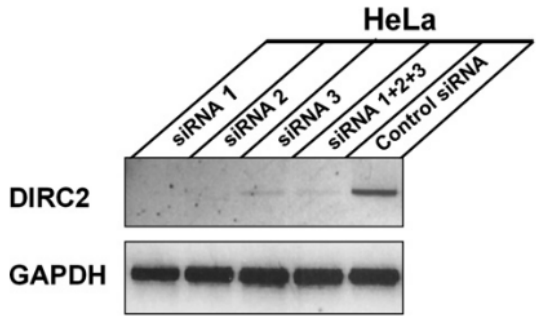

Figure S1 Expression of DIRC2 in HeLa cells and validation of DIRC2 siRNA

HeLa cells were transfected with three different siRNAs targeting DIRC2, either indidually or in combination (siRNA 1 + 2 + 3) or with non-targeting control siRNA. Total RNA was isolated and transcripts of *DIRC2* and *GAPDH* as a control were amplified by RT (reverse transcription)–PCR. In agreement with the Western blot shown in Figure 4(A) of the main paper, this confirms the expression of endogenous DIRC2 in HeLa cells. In cells that had been transfected with siRNA directed against DIRC2, the level of *DIRC2* mRNA appeared to be strongly reduced which validates the effectiveness of the siRNA.

[1] These authors contributed equally to this work.
[2] Present address: Department of Mathematics and Sciences, University of Mataram, Mataram, Indonesia.
[3] Correspondence may be addressed to either of these authors (baschroeder@biochem.uni-kiel.de or psaftig@biochem.uni-kiel.de).

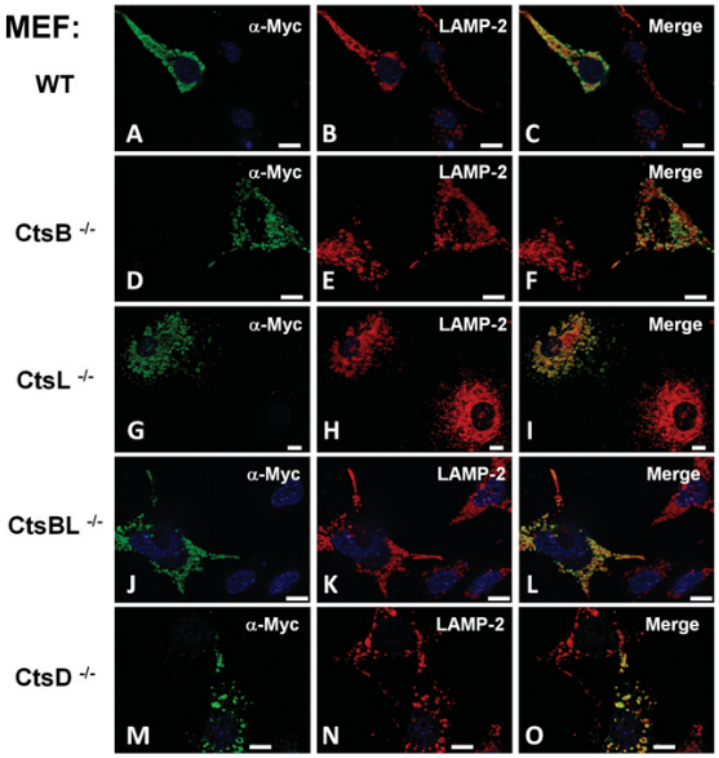

Figure S2 Lysosomal localization of overexpressed DIRC2 in protease-deficient MEFs

MEFs derived from wild-type mice (WT) or mouse strains deficient in one or more lysosomal proteases (cathepsin B, CtsB$^{-/-}$; cathepsin L, CtsL$^{-/-}$; cathepsin B and L, CtsBL$^{-/-}$; and cathepsin D, CtsD$^{-/-}$) were transiently transfected with DIRC2–3× Myc-pcDNA3.1/Hygro +. Cells were fixed 48 h after transfection. The distribution of triple-Myc-tagged DIRC2 was monitored by indirect immunofluorescence using an anti-Myc antibody. Lysosomes were visualized by co-staining of the lysosomal marker protein LAMP2. In all cell lines overexpressed DIRC2 was targeted to lysosomes, as indicated by its co-localization with LAMP2.

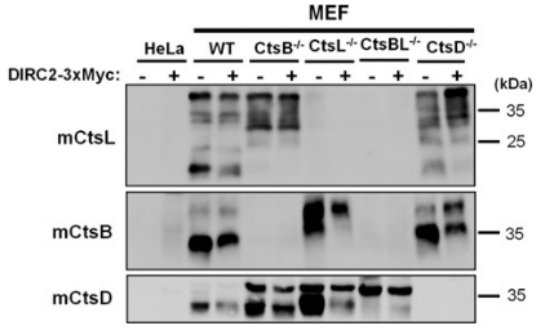

Figure S3 Cathepsin expression control in knockout MEF cell lysates

HeLa cells, as well as MEFs derived from wild-type mice (WT) or mouse strains deficient in one or more lysosomal proteases (cathepsin B, CtsB$^{-/-}$; cathepsin L, CtsL$^{-/-}$; cathepsin B and L, CtsBL$^{-/-}$; and cathepsin D, CtsD$^{-/-}$) were transiently transfected with DIRC2–3× Myc-pcDNA3.1/Hygro + (+) or empty vector (−). Cells were harvested 48 h after transfection and aliquots of total lysates (20 μg of protein) were subjected to SDS/PAGE and Western blot analysis. As a control, the lysates from the experiment depicted in Figure 7 of the main text were also analysed with antibodies for the presence of endogenous murine cathepsin L (mCtsL), cathepsin B (mCtsB) and cathepsin D (mCtsD). The molecular mass in kDa is indicated on the right-hand side.

Received 25 January 2011/6 May 2011; accepted 22 June 2011
Published as BJ Immediate Publication 22 June 2011, doi:10.1042/BJ20110166

C1 Turnitin L. R. Telly Savalas

ORIGINALITY REPORT

14%	12%	11%	%
SIMILARITY INDEX	INTERNET SOURCES	PUBLICATIONS	STUDENT PAPERS

PRIMARY SOURCES

1	d-nb.info Internet Source	4%
2	www.jove.com Internet Source	2%
3	rupress.org Internet Source	1%
4	Jonatan Sánchez, Ana Talamillo, Monika González, Luis Sánchez-Pulido et al. " Sal and Salr are transcriptional repressors ", Biochemical Journal, 2011 Publication	1%
5	Bernd Schröder, Christian Wrocklage, Andrej Hasilik, Paul Saftig. "Molecular characterisation of 'transmembrane protein 192' (TMEM192), a novel protein of the lysosomal membrane", Biological Chemistry, 2010 Publication	1%
6	www.pnas.org Internet Source	1%

7	Jörg Behnke, Janna Schneppenheim, Friedrich Koch-Nolte, Friedrich Haag, Paul Saftig, Bernd Schröder. "Signal-peptide-peptidase-like 2a (SPPL2a) is targeted to lysosomes/late endosomes by a tyrosine motif in its C-terminal tail", FEBS Letters, 2011 Publication	1 %
8	www.oncotarget.com Internet Source	1 %
9	mcb.asm.org Internet Source	1 %
10	s3.amazonaws.com Internet Source	1 %

Exclude quotes	On	Exclude matches	< 1%
Exclude bibliography	On		